2016

Adams As Potential Regulators of Stem Cell Quiescence in the Olfactory Epithelium

Elaine Elizabeth Orendorff
Loyola University Chicago

LOYOLA UNIVERSITY CHICAGO

ADAMS AS POTENTIAL REGULATORS OF STEM CELL QUIESCENCE IN THE OLFACTORY EPITHELIUM

A THESIS SUBMITTED TO

THE FACULTY OF THE GRADUATE SCHOOL

IN CANDIDACY FOR THE DEGREE OF

MASTER OF SCIENCE

PROGRAM IN BIOLOGY

BY

ELAINE E. ORENDORFF

CHICAGO, IL

DECEMBER 2016

ACKNOWLEDGMENTS

I would like to thank my advisor Dr. Jessica Brann for her unwavering support and expert guidance, for giving me room to grow, and for inspiring me to be a better student and researcher. I also want to thank my committee members, who each in their own way helped me to develop my thesis. Dr. William Rochlin, who taught me valuable lessons in developmental biology and in how to present research findings. Dr. Stefan Kanzok, who shared his knowledge regarding gene regulation and the fundamentals of RT-qPCR. The input from all three professors has improved the quality of my work. I would also like to thank members of the Brann lab: Lucas Klemm, a former undergraduate, who first analyzed the literature for genes of interest; Paulina Lis, our lab technician, who keeps the lab running smoothly and ran Western blots on my behalf; Mary Makarious, an undergraduate, who helped me to prepare slides and perform IHC; as well as the other Brann lab members, who have been cheerful and cooperative teammates. I want to thank the members of the Biology Department: Dr. Theresa Grande, Dr. Timothy Hoellein, Audrey Berry, Frank Inglima, and Virginia Lorenzo for their administrative support during my time in the program. I am grateful to the Graduate School for providing fellowship funding, which has allowed me to pursue this master's degree. Finally, I would like to thank my family for their constant love and support as I find my way in the world.

TABLE OF CONTENTS

LIST OF TABLES

LIST OF FIGURES

ABSTRACT

I demonstrate that a member of the protein family A Disintegrin and Metalloprotease (ADAM), ADAM23, is expressed in the olfactory epithelium (OE) and may inhibit neural progenitor cell (NPC) proliferation. I generated a list of ten gene candidates and selected ADAM23 for further study, based on its conserved protein structure and accumulating evidence for its role in cell cycle progression of proliferative cells. I next determined ADAM23 protein localization using immunohistochemistry and measured both mRNA and protein expression post-lesion with RT-qPCR and Western blot. ADAM23 is expressed in multiple cell types of the OE, including glial Sustentacular (Sus) cells and neurons. There are four splice variants present in the OE, and mRNA expression decreases three to four-fold post-lesion but recovers to pre-lesion levels within two weeks ($p<0.05$, ANOVA). ADAM23 is poised to regulate NPC quiescence through contact with Sus cell end-feet. It may also facilitate important Sus:neuron interactions.

CHAPTER ONE

INTRODUCTION

Regeneration in the Nervous System

Mammals have a limited capacity for repair of their damaged tissues. We cannot regrow limbs or eyes like some lower vertebrate species. Furthermore, the capacity to regenerate decreases with age even for proliferative cells of the skin and gut, as demonstrated by thinning and scarring of the epithelial tissue (Rando et al, 2012). Nervous tissue is not as easily repaired and injuries sustained to the brain or spinal cord are often life-altering. Nonetheless, adult neurogenesis can and does occur in three primary areas of the mammalian nervous system: the olfactory epithelium (OE), the subventricular zone (SVZ), and the subgranular zone (SGZ) (Riddle and Lichtenwalner, 2007). However, only the OE produces afferent excitatory projection neurons throughout life (Whitman and Greer, 2009). Learning more about the mechanisms within the OE that promote regeneration could be applied to the repair of other nervous system tissues in the future.

First, it is important to consider the similarities and differences between neurogenesis that occurs during development as opposed to that during regeneration. Stem cell populations in adult tissues must remain undifferentiated and self-renew for an extended period of time, but not be permitted to generate new cells in an uncontrolled manner. They must be responsive to extracellular signals upon injury in order to generate multiple tissue-specific cell types as needed; and when repair is finished they must re-

enter a state of quiescence.

Stem cell maintenance and activation

Between stem cell niches there are certain common and divergent characteristics. It is common for stem cells to be adherent to a basal lamina, and in close proximity to the vasculature such that they respond to cytokines, chemokines, and other circulating factors (Ovadia et al, 2013; Putnam, 2014). NPCs of the SVZ and OE are similar in this way but differ in origin and morphology. NPCs of the SVZ are derived from the neural plate and resemble radial glia, whereas NPCs of the OE are derived from the neural placode and are flat or rounded in shape, although they appear to adopt a radial phenotype upon injury (Suzuki et al, 2013; Barry et al 2014; Brann et al, 2015). These populations, respectively, produce interneurons or projection neurons throughout life. SVZ neuroblasts migrate through the rostral migratory stream to the olfactory bulb (OB) where they differentiate and integrate as interneurons of the periglomerular or granule cell layers (Lledo et al, 2008). The cell bodies of newborn neurons in the OE migrate only a short distance apically towards the nasal cavity, before extending long axons to the appropriate location in the OB. Regeneration in the OE is of interest because of the projection neurons produced, as well as for the ease of access to NPCs in the nasal cavity for biopsy and possible transplantation.

Cell Types and Organization of the Olfactory Epithelium

Two different populations of NPCs, horizontal basal cells (HBCs) and globose basal cells (GBCs), give rise to all other cell types of the OE (reviewed in Brann and Firestein, 2014). As with other epithelia, the OE is made up of distinct cell layers that can be distinguished by cell morphology and cell specific markers (Figure 1). HBCs adhere to

the basal lamina, proliferate slowly, and self-renew (Mackay-Sim and Kittel, 1991). They express Intercellular Adhesion Molecule 1 (ICAM1), Cytokeratin 5 (KRT5), and an isoform of Tumor Related Protein (ΔNp63).

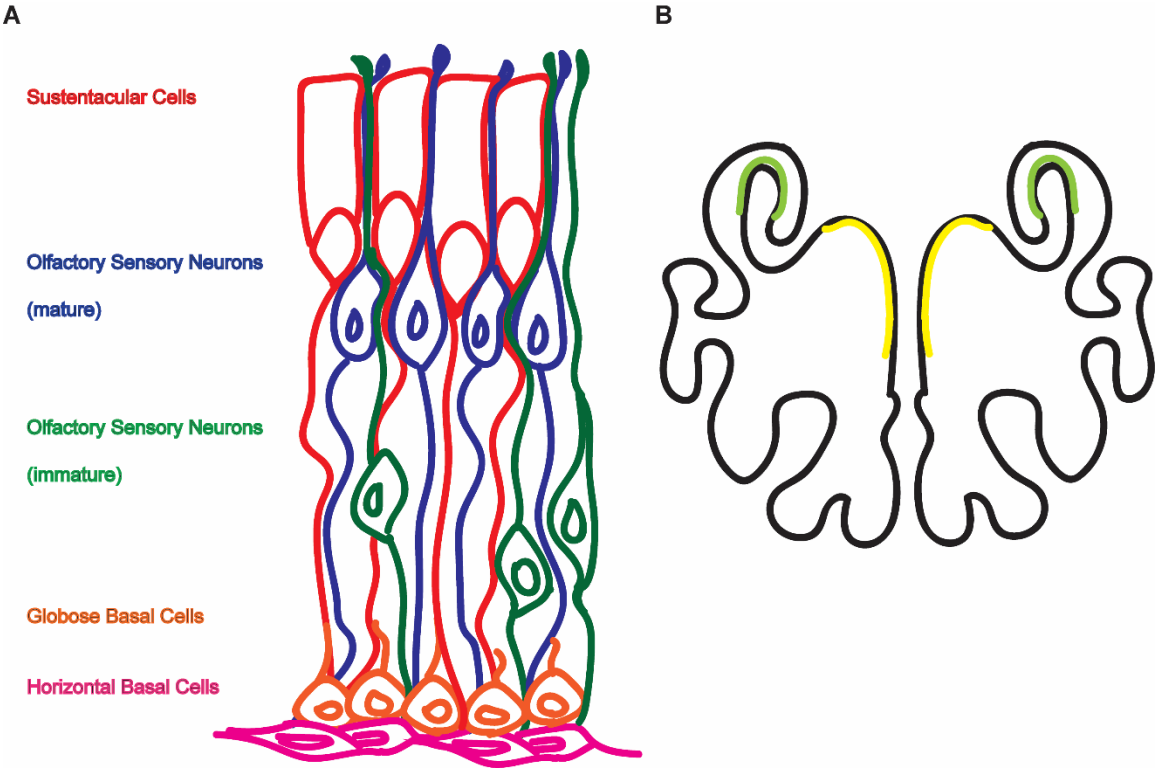

Figure 1. Cell Layers of the Olfactory Epithelium and Coronal Tissue Section. (A) Horizontal basal cells (HBCs; pink) and Globose basal cells (GBCs; orange) form distinct cell layers and give rise to immature olfactory sensory neurons (OSN_i; green) and sustentacular cells (Sus; red). The mature OSNs (OSN_m; blue) have dendrites that terminate in cilia (where odorant receptors and the sensory signal transduction apparatus are expressed) exposed to the nasal passage. OSN_m also have axonal projections to the olfactory bulb (OB). Sus cells provide support to the neurons and are a type of glial cell. (B) The OE lines the nasal cavity and is supported by a complex boney structure to increase surface area for odorant detection. Looking at a coronal section, the epithelium wraps around in what are called turbinates and also along the middle structure called the septum which curves into the dorsal recess. The dorsal recess/septum (yellow) will be compared to turbinate (light green) in this study. The neurons in the dorsal recess/septum express more evolutionarily ancient odorant receptors compared to other zones of the OE.

GBCs are restricted to a layer directly above the HBCs and share many similarities with embryonic progenitor cells. They express transcription factors associated with neural differentiation including: Achaete-Scute Homolog 1 (ASCL1) and Neurogenin 1 (NGN1). Most GBCs cycle rapidly, generating new cells, some of which mature and integrate into the tissue, while the remainder undergo apoptosis. There is however a small segment of the GBC population that progresses more slowly through the cell cycle to self-renew (Jang et al., 2014). Down-regulation of ΔNp63 transitions HBC to GBC, changing the reserve status or quiescence of the cell (Schnittke, 2015).

Cells produced by NPCs migrate apically as they differentiate into olfactory sensory neurons (OSNs) or glial sustentacular cells (Sus). Immature OSNs (OSN_i) express many factors common to immature neurons such as Growth Associated Protein 43 (GAP43) and Doublecortin (DCX); mature OSNs (OSN_m) are distinguished by expression of the signal transduction machinery necessary for odorant detection including: Adenylate Cyclase III (ADCY3), Olfactory G-protein (GNAL/G_{olf}), Cyclic Nucleotide Gated Channel Alpha 2 (CNGA2), and also by Olfactory Marker Protein (OMP). OSN cell bodies are in the middle layers of the epithelium and extend dendrites to the nasal cavity. Sus cells express Epithelial-Cadherin (ECAD), Cytokeratin 18 (CK18), as well as factors shared with NPCs, such as Sex Determining Region Y-Box 2 (SOX2). Sus have apical cell bodies and send projections basally, terminating in end-feet that surround the NPC populations (Figure 1).

Injury Response in the Olfactory Epithelium

There is regular turnover of OSNs in the OE, but the extent to which regeneration is possible after severe damage is an object of intense study. In general, the olfactory

sensory circuit can be recapitulated and function restored as long as the OB target remains intact. All neurons expressing the same odorant receptor synapse with mitral cells in the OB in spherical structures known as glomeruli (reviewed in Mombaerts, 2006). When the olfactory bulbs are surgically removed (olfactory bulbectomy or OBX), HBCs may or may not be recruited, but GBCs actively generate new OSN_i that, when unable to synapse onto the OB also degenerate and a repetitive cycle begins (Leung et al, 2007; Iwai et al, 2008).

Chemical lesion on the other hand, commonly experimentally induced by exposure to methyl bromide gas or the anti-thryroid drug methimazole, spares the OB but induces massive cell death in the OE. For this reason, it is thought that HBCs are recruited to reconstitute the depleted cell types of the OE. Basal cell proliferation peaks approximately five days post-lesion, as indicated by bromodeoxyuridine (BrdU) mediated birth dating and by the thickness of the HBC layer which expands to two to three times its usual thickness (Leung et al, 2007), while at this time OSN marker labeling is at a low. The numbers of OSN_i and OSN_m start to increase after seven days post lesion and cell proliferation returns to control levels in four to six weeks. It takes about eight weeks for recovery to be complete (Schwob et al, 1995).

A Disintegrin and Metalloprotease (ADAM) Family

Changes in gene expression during critical periods of NPC activity may permit insight into what permissive factors are present in the OE that support neural regeneration. For the following project, I identified gene candidates which I hypothesized to be important for NPC maintenance and activation based on their expression in the literature. A member of A Disintegrin and Metalloprotease (ADAM) family, ADAM23,

was selected for further study. ADAMs are cell-signal, cell-adhesion, signal transduction proteins involved in processes such as proliferation, differentiation, and guidance, but they have not been studied to a great extent in the OE.

Conserved Protein Domains

ADAM1 and ADAM2, also known as Fertilin-alpha and beta, are transmembrane proteins necessary for sperm migration and sperm-egg binding respectively. They share conserved domain structures with a family of soluble proteins found in snake venom called the *Metalloproteinase, Disintegrin-like, Cysteine-rich* (MDC) family. Snake venom MDCs digest extracellular matrix (ECM) proteins, similar to the cell secreted Matrix Metalloproteinases (MMPs), but their effect is hemorrhagic, breaking down the basal lamina of blood vessel walls. The disintegrin domain binds integrins and prevents blood coagulation (Kamiguti et al, 1998). The ancient Hebrew name for the first man, ADAM, was therefore chosen, not only as an acronym for two specific protein domains, but as a nod to the role of some ADAMs in male fertility and their connection to snakes (Wolfsberger et al, 1995).

In addition to the conserved metalloprotease and disintegrin domains, ADAMs have epidermal growth factor (EGF)-like and cysteine-rich domains, a transmembrane region, and a cytoplasmic tail (Figure 2A). ADAMs with a functional metalloprotease domain act as ectodomain sheddases (Figure 2C). ADAM10 and ADAM17 notably cleave cadherins, TNF-alpha and Notch receptors (Reiss et al, 2005; Hikita et al, 2009; Bozkulak et al, 2009). Catalytically inactive ADAMs include some primarily expressed in the testis (ADAM2, 3, 4, 5, 6, 18, 29, 32) as well as those expressed in the brain (ADAM11, 22, 23) (Choi et al, 2004; Sagane et al, 1998). These act primarily as cell-

adhesion proteins. The disintegrin domain is known to bind to integrins, to leucine rich glioma inactivated (LGI) proteins (Sagane et al, 2008; Seppala et al, 2011), and evidence suggests interactions with other unidentified binding partners (Bridges, 2008). The disintegrin domain is important for cell adhesion (Cal et al, 2000), guidance (Huang et al 2003), proliferation (D'abaco et al 2006), and differentiation (Lafuste et al, 2005; Kawaguchi et al, 2003). Both the metalloprotease and disintegrin binding sites are inactive until the prodomain is cleaved. The EGF-like domain is likely involved in protein-protein interactions and may help ADAMs to form heterodimers. The cysteine-rich domain has been shown to facilitate cell-adhesion through interactions with syndecans and fibronectin (Iba, 2000; Gaultier 2002).

A

B

```
Adam23 splice variants
V2 (beta)   781 GPK|VNMATSRLIGAVAGTVLALGVIFGGTGWGIE|NVKKRRFDPTQQGPI--------   829
X1 (alpha)  781 GPK|GPSATNLIIGSIAGAILVAAIVLGGTGWGFK|NVKKRRFDPTQQGPI--------   829
X2 (gamma)  781 GPK|ETSRRGDS-IPLSKAPSESSALEECHL------ALLGSGNDMFSAMLPELLSL-   829
V1          781 GPKGLYDSGFRSLQIIHLPSPTAAVIHFHSFRRRHTGIYPFATEMRHPVCTTLSEAY    837
X3          781 GPKEHLSLKNLKI---------IILSQC-----------------------------   799
                ***                     :
```

C

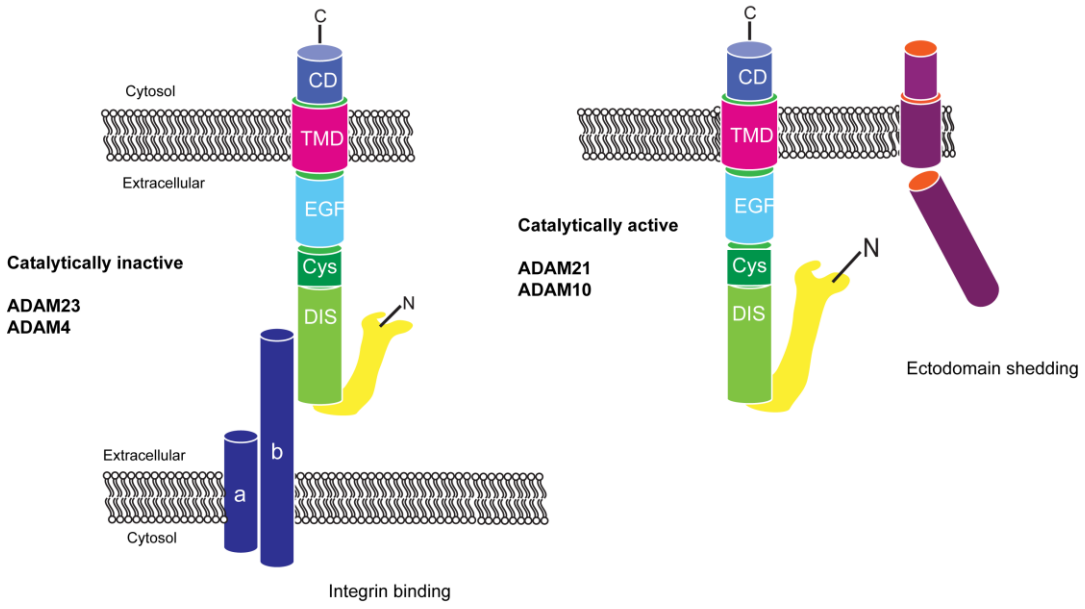

Figure 2. ADAM Family of Proteins. (A) Adam domains common to all family members. Signal peptide (Sig, red), Prodomain (Pro, orange) which is cleaved prior to insertion in the membrane, Metalloprotease (Met, yellow) which depending on the ADAM may or may not be catalytically active, Dinsintegrin (Dis, light green) binds to integrins and other proteins, Cystein rich domain (Cys, dark green) involved in protein binding, Epidermal growth factor-like (EGF, light blue) domain involved in protein binding, Transmembrane (Trans, pink) region spanning the membrane, Cytoplasmic tail (Cyt, periwinkle) for signal transduction. (B) Predicted *Adam23* splice variant sequences in mouse and their alignment. The identified transmembrane regions are highlighted in pink. (C) The linear protein is processed before insertion in the membrane. The Dis domain binds to integrins (dark blue). Those ADAMs with a functional Met domain cleave ectodomains (purple) from proteins such as TNFα and Notch receptors.

Between members of the ADAM family there is about 30% protein sequence identity across all conserved domains. For some ADAMs there are multiple splice variants which have identical extracellular domains but different transmembrane regions and cytosolic tails. ADAM23 exhibits four primary splice variants (Figure 2B), likely with different roles in signaling. ADAMs are involved in both "forward" outside-in and "reverse" inside-out signaling (Tanaka et al, 2004). The cytosolic tail interacts with proteins via a sarcoma homology 3 (SH3) docking sequence (Kleino et al, 2015). It activates Phosphoinositide 3 Kinase (PI3K) (Kang et al, 2000; Kang et al, 2001), Focal Adhesion Kinase (FAK) (Böhm et al, 2013; Fried et al, 2015), and Extracellular-Signal Regulated Kinase (ERK1/2) (Sun et al, 2010) pathways that are involved in cell cycle regulation and cytoskeletal reorganization.

ADAMs of Interest in the Olfactory Epithelium

Each ADAM possesses an integrin binding domain and a transmembrane region facilitating signal transduction. Protein localization studies show integrins, which regulate cell interactions and mitosis, present in both HBCs and Sus cells (Carter et al, 2004). ADAMs present in the OE could potentially bind integrins on either cell type.

HBCs are flattened on the basal lamina until they start to proliferate and move apically, becoming more rounded in shape. Given that ADAMs are tied to both cytoskeletal reorganization and cell cycle progression, they are a likely candidate for HBC regulation.

For the most part ADAMs in the OE have not been studied. Previous work has shown the catalytically active ADAM10 protein is localized to neurons and basal cells (Yavari et al, 1998). In another study, ADAM21 was shown to be in immature OMP-negative axons innervating the olfactory bulb, and metalloprotease inhibitors were labeled in the periglomerular area indicating that ADAM21 could be important for OSN axon guidance. In the SVZ, ADAM21 is expressed in cells of the subependymal and ependymal layers, in potential NPCs and glial cells that have projections onto blood vessels (Yang et al 2005).

This project is the first to examine the expression and regulation of a catalytically inactive ADAM in the OE. ADAM23 was identified from three independent microarray experiments of a recovery time-series post-bulbectomy (Heron et al, 2013; Shetty et al, 2005; Borders et al, 2007). I hypothesized that genes significantly different in expression days one through five of the series could be involved in activation of the basal populations. ADAM23 is essential for neural development. Knockout mice exhibit severe ataxia and tremor, and die within two weeks of birth (Mitchell et al, 2001). ADAM23 has been studied in pluripotent stem cells as an integral part of stem cell maintenance. P19 carcinoma cells usually require both cell aggregation and retinoic acid (RA) for induction of a neural cell fate decision. When ADAM23 was knocked down in the embryonic stem cell line, neural differentiation occurred without induction by RA (Sun et al, 2007; Wang et al, 2012). Knockdown arrested progression through the cell cycle, keeping a higher

percentage of cells in the G1 phase, a key step before differentiation. The inhibitory effect of ADAM23 on differentiation was recapitulated by application of the purified GST-tagged disintegrin domain to ADAM23 knockout cells, indicating that signal transduction occurred through ADAM23's interaction partner, likely a beta-1 integrin (Wang et al, 2012). ADAM23's role in cell cycle arrest is further demonstrated by its frequent silencing in cancer cells, promoting metastasis (Verbisck et al, 2009). ADAM23 could likewise regulate NPC activation and differentiation in the OE.

Rationale for the Proceeding Experiments

After identifying *Adam23* as a gene of interest for NPC regulation, I designed primers to detect the presence or absence of transcript in OE tissue. Having confirmed transcription, I focused on determining the cellular localization of ADAM23 protein. I then asked whether *Adam23* transcript and protein levels are dynamically regulated during postnatal development, as proliferation declines, or during recovery from injury, as proliferation is induced. If ADAM23 were important for maintaining a quiescent NPC population in the OE, then it should be stably expressed between postnatal days 30-60 and upon injury it should be down-regulated one to three days following injury. As will be discussed, my results provide evidence for ADAM23's potential role in inhibiting proliferation through cell-cell interactions.

CHAPTER TWO

MATERIALS AND METHODS

Animal Care & Sources

All experiments were done in compliance with Loyola University of Chicago Institutional Animal Care and Use Committee guidelines in C57BL/6, SVE/129 wild-type inbred mice, or OMP-GFP heterozygotes ages 4-12 weeks. The OMP-GFP mice are a targeted knockout reporter strain with 129P2/OlaHsd background and high expression of GFP (Potter et al, 2001). Mice were anesthetized by intraperitoneal injection with a mixture of ketamine/xylazine (0.05-0.15 mL of 18 mg/mL, and 2 mg/ml, respectively).

Immunohistochemistry (IHC)

Mice were anesthetized then perfused transcardially with heparinized PBS (4 U/mL) and 3% PFA/0.1% glutaraldehyde in 0.1M PB. Tissue was decalcified in 0.5 M EDTA (pH 8.0), cryopreserved in 30% sucrose, and embedded in Tissue-Tek OCT (Sakura Finetek, Torrance, CA). Cryosections (12 µm) were warmed 10 min, hydrated in PBS 10 min, blocked in 3% H_2O_2 30 min, Avidin/Biotin block 10 min each (Invitrogen, Carlsbad, CA), and 10% Normal Donkey Serum (NDS)/0.1% Triton in PBS for 1 hr, followed by incubation with primary antisera recognizing ADAM23 (SC50482, 1:200, Santa Cruz, Dallas, TX), ICAM (AF583, 1:100, requires antigen retrieval 5 min in steamer with sodium citrate before block, RD Biosystems, Minneapolis, MN), ECAD (U3254, 1:500, Sigma Aldrich, St. Louis MO), or DCX

(SC8066, 1:200, Santa Cruz) overnight at 4°C. After 16-18 hr primary incubation, tissue sections were exposed to secondary antisera 90 min at room temp (donkey anti-rabbit biotin 1:500, donkey anti-goat 488 1:300, goat anti-rat 633 (1:750) extra block step with 10% Normal Goat Serum, donkey anti-goat 633 1:750). TSA amplification for ADAM23 was done according to the manufacturer's protocol (TSA kit #24 1:100, 1:100, Molecular Probes, Eugene, OR). Slides were rinsed after secondary incubation 3 x 5 min with PBS and incubated with horseradish peroxidase conjugated anti-biotin 1:100 in 10% NDS/ 0.1% Triton in PBS for 60 min. Slides were rinsed 3 x 5 min with PBS and incubated with tyramide-568 1:100 in amplification buffer with 0.0015% H_2O_2 for 10 min. Slides were then rinsed 3 x 5 min in PBS. DRAQ5 or TOTO diluted 1:10K in PBS was applied for 15min before rinsing again 3 x 5 min. Slides were cover-slipped with Vectashield (Vector Laboratories, Burlingame, CA) and images acquired on an Olympus Fluoview 1000 confocal microscope (Olympus America, Center Valley, PA) then subsequently analyzed with Image J software (NIH, Bethseda, MD) and the UCSD plugin.

Immunocytochemistry (ICC)

OE tissue was dissected on ice in Earle's Balanced Salt Solution (EBSS) and broken up with forceps. The tissue was dissociated using a Papain Dissociation System (Worthington Biochemical Corp, Lakewood, NJ) according to the manufacturer's instructions. Incubation with papain and a DNase enzyme in EBSS was for 45-60 min on a rocker at 37°C speed 90. The cells were triturated, centrifuged, re-suspended in EBSS with ovomucoid papain inhibitor, and plated onto laminin coated coverslips. Cultures were kept at 37°C in a CO_2:O_2 incubator for 60 min before fixing with 4% PFA in 0.1M PB for 15 min. Cells were blocked in 5% NDS/0.1% Triton for 30 min, incubated with

primary antisera in PBS for 1 hr at room temperature or overnight at 4°C (rabbit anti-ADAM23 1:50), secondary for 45 min at room temp (donkey anti-rabbit 568 1:750), and DRAQ5 1:10K. Slides were cover-slipped with Vectashield and images acquired on an Olympus Fluoview 1000 confocal microscope, then analyzed with the Fiji Image J Package and the Analyze Particles plug-in (Schindelin et al, 2012).

ICC Statistical Analysis

Using the Analyze Particles plug-in, I made a mask for each channel which could be applied to the others for detection of overlapping particles. The number of cells co-labeled for a given set of markers was divided by the number of cells positive for a single marker. This gave a proportion of co-labeled cells. Proportions can be either log or arcsinsqrt transformed to obtain a Gaussian distribution. There are often zeros in cell count data which makes the arcsinsqrt transformation a better option. I performed a student's t-test using GraphPad Prism 7 (GraphPad Software Inc, La Jolla, CA).

Lesion of the Olfactory Epithelium

Mice were administered either 50 mg/kg Methimazole (Sigma) or the same volume per weight of saline in a randomized manner via intraperitoneal injection. Mice were monitored daily for a week after injection for weight loss induced by drug administration and were euthanized if 20% or greater weight loss was observed.

Microarray Data Mining

The Gene Expression Omnibus (GEO) database is a repository of high-throughput genomics data supplied by members of the scientific community and made available to the public. Three microarray studies from the database were selected and analyzed (Heron et al, 2013; Shetty et al, 2005; Borders et al, 2007) with GEO2R (Edgar et al,

2002), an online tool which compares user-selected groups with correction for multiple-tests. All three studies examined the time-course of recovery in mouse OE, following olfactory bulbectomy. From a long list of genes, found to change in expression early post-bulbectomy, ten short-list candidates were selected using the MGI Gene Ontology tool (Jackson Labs, Barharbor, ME). These genes were involved in processes such as cell-signaling, signal transduction, proliferation, differentiation, and cell-adhesion in other tissues.

Primer Design

Target sequences were obtained from the NCBI nucleotide database. Primers were designed using NCBI Primer Blast with a product size between 110-150 bp and melt temp between 57-63°C. When possible primers were separated by at least one intron on the genomic DNA. Primers were blasted against the genome reference assembly to check for specificity to mRNA sequences. Primers were analyzed using Oligoanalyzer before ordering (Integrated DNA Technologies Inc, Coralville, IA) where ΔG was no less than -10 kcal/mol for hairpin, self-dimer, and heterodimer formation.

Reverse Transcriptase Polymerase Chain Reaction (RT-PCR)

OEs were rapidly dissected and placed in RNAlater (Qiagen, Valencia, CA) and stored 24 hrs after isolation at -80°C until homogenized using RNase-Free Red Bead Lysis Kit tubes and a Bullet Blender (Next Advance, Averill Park, NY). RNA was extracted using a RNeasy Micro Kit (Qiagen) according to the manufacturer's protocol. Excess RNAlater was removed from tissue, and tissue was weighed and divided with less than 5 mg per Red tube. To each tube 1ml RLT buffer from the RNeasy kit and 10 μL β-mercaptoethanol was added before blending 3 min on speed 8 at 4°C. Samples were

centrifuged 3 min at 14,000 rpm and the supernatant removed. 700 μL of 70% ethanol was added to the supernatant, mixed by pipetting, and transferred to a RNeasy MinElute spin column. The columns were centrifuged 15 sec at 13,400 rpm. The flow through was collected and each column placed in a new collection tube. Each column was washed with 350 μL of Rneasy RW1 and columns were centrifuged for 30 sec at 13,400 rpm. From the RNeasy kit 3,220 μl of Buffer RDD was added to 460 μL of DNase1 and mixed by inversion, then 80 μl of this DNase solution was added directly to the membrane of each column and allowed to incubate 15 min at room temperature, followed by a wash with 350 μL of Rneasy RW1 buffer, and centrifugation for 30 sec at 13,400 rpm. The flow through was discarded and 500 ul of RNeasy RPE buffer working stock was added to each column and centrifuged 30 sec at 13,400 rpm. Flow through was discarded and 500 ul 80% ethanol was added to the column and centrifuged 2 min at 13,400 rpm. Flow through was discarded and columns were dried before adding 14 ul of RNase free water to each membrane and centrifuged 1 min at 13,400 rpm. The eluted RNA samples were then stored at -80°C. RNA quality was verified using a Nanodrop spectrophotometer to obtain a 260/280 nm ratio of approximately 2.0 (Thermo Fisher, Waltham, MA). A Superscript III First Strand Synthesis Kit (Thermo Fisher) was used to generate cDNA from purified RNA. The presence or absence of target transcripts was determined by running PCR (2x Mastermix: Promega, Fitchburg, WI) at 95°C for 3 min, followed by 30 cycles of 95°C for 30 sec, 60°C for 30 sec, 72°C for 45 sec, then 72°C for 7 min on a T100 thermocycler (Bio-Rad, Hercules, CA). The PCR product was run on a 20% acrylamide gel in 1x TAE at 100V for 45 min and imaged with an Odyssey FC imaging system (LI-COR, Lincoln, NE).

Real Time Quantitative Polymerase Chain Reaction (RT-qPCR)

Olfactory epithelia were dissected and stored as described above until homogenized using Tri-reagent RT (MRC Gene, Cincinnati, OH). Tissue was weighed to be less than 100 mg before blending in 1 ml Tri-reagent RT in the Bullet blender on speed 8 for 5 min at room temperature. The samples were then centrifuged at 14,000 rpm for 3 min at 4°C. The supernatant was transferred to a new tube and 50 μl 4-bromo anisole was added for phase separation after shaking 15 sec. Samples were centrifuged 12,000 g for 15 min at 4°C. The aqueous phase was transferred to a new tube for a second phase separation with another 800 μl Tri-reagent RT and 50 μl 4-bromo anisole. The interphase and phenol phase were stored at 4°C for protein isolation 24 hrs later. After the second separation the aqueous phase was transferred to a new tube and 800 μl isopropanol was added to precipitate the RNA. The samples were allowed to set for 10 min at room temperature then centrifuged 12,000 g for 5 min at 4°C. The supernatant was discarded and the pellet was washed by adding 1 ml 75% ethanol and vortexed before centrifuging 12,000 g for 5 min at 4°C. The supernatant was discarded and the wash step repeated before dissolving the pellet in 600ul water and storing at -80°C.

A High Capacity RNA-to-cDNA Kit (Applied Biosystems, Foster City, CA) was used to generate cDNA. To optimize the PCR reaction, to avoid primer dimer formation as seen by gel electrophoresis, the Amplitaq Gold Fast PCR mastermix was used (Applied Biosystems, Foster City, CA)) at 95°C for 10 min, followed by 35 cycles of 96°C for 3 sec, 60°C for 3 sec, 68°C for 5 sec, and then 72°C for 10 sec. To optimize primer concentrations for a reaction efficiency of 100 ± 10%, a five-point dilution of sample RNA was used to generate cDNA, and standard curves for each primer pair were

run using Power-Up Syber Green Mastermix (Applied Biosystems) on a Step-One Plus Real-Time PCR machine (Applied Biosystems) at 50°C for 2 min, followed by 40 cycles of 95°C for 2 min and 60°C for 30 sec, then 95°C for 15 sec, 60°C for 1 min, and 95°C for 15 sec. For relative quantification of the genes of interest two house-keeping genes were selected to use in combination using Normfinder (Andersen et al, 2004). A reaction plate, with three genes and three technical replicates for each experimental condition, was run for each biological replicate using the Power-UP Syber and Step-One Plus machine. The primer sequences and concentrations can be found in Table 1.

Table 1. RT-qPCR Primers

Gene	Forward	Reverse	µM	bp
Pgk1 NM_008828.3	TGGTGGGTGTGAATCTGCC	ACTTTAGCGCCTCCCAAGATA	50	124
Tfrc NM_011638.4	CATTGCGGACTGTAGAGGCG	TTGCCGAGCAAGGCTAAACC	50	134
Adam23v2 NM_011780.2	CCAGTTCGGAACCCCAACC	CTCCTCTTCTTGACGTTTTTAAATCCC	100	150
Adam23x1 XM_006495969.1	GGGTGATTTTTGGAGGCACAG	CCAGAACCCAACAGTGCAAG	100	128
Adam23x2 XM_006495970.1	GGTGTGTAGCAACGAAGCCA	CTTCTTGACGTTTCCTTAGGGC	100	126
Adam23v1 NM_001177600.1	GCCACGGGGTGTGTAGCA	GCAGTGATCTAAAACCGGAATCAT	100	150
Adam23x3 XM_006495971.1	CCAGTTCGGAACCCCAACC	GTATTCCAGGCAGGCAGATGA	100	124
Adam4 NM_009620.1	AGCAATTCCTCCACCTCAGT	CGGGGACAGTATGCAGGTTC	50	136
Adam21 NM_020330.4	GCCTGCACAGAGGTTATGGA	GCCCAGCTATGAGCAGACAA	50	129
Adam10	ATGGTGTTGCCGACAGTGTTA	GTTTGGCACGCTGGTGTTTTT	50	151
Adam2 NM_009618.2	CACAGCGGATCGTCTCTCAC	GCATTTGCCAGTCCAATCAACT	50	127
Adam2x1 XM_006518439.1	CCCCCAACTGCCCTGTAGA	ATTTCTCACGAGTGCCTTCTGT	50	148

ΔNp63 NM_001127265.1 NM_001127264.1 NM_001127263.1 NM_001127262.1 NM_011641.2	TGTACCTGGAAAACAATGCCC	CGCTATTCTGTGCGTGGTCT	50	141
*Ascl1** NM_008553.4	TCGTTGGCGAGAAACACTAA	AGGAACAAGAGCTGCTGGAC	50	120
Ecad NM_009864.3	CCGTCCTGCCAATCCTGATG	TGCCCTCGTAATCGAACACC	100	116
*Gap43** NM_008083.2	CTGCTGCTGTCACTGATGCT	GGCTTCGTCTACAGCGTCTT	50	131
*Omp** NM_011010.2	GTCCAGAACCACGTTCCAGT	GGAGAAGAAGCAGGATGGTG	100	112

*(Fletcher, 2011)

RT-qPCR Data Analysis

The output of the StepOne Plus software version 2.3 calculated differences in cycle times (ΔCT) between a gene of interest and the mean of two reference genes *Pgk1* and *Tfrc*. I transformed these into relative expression values $2^{\wedge-\Delta CT}$ by assuming 100% reaction efficiency. I then normalized each lesion condition to a saline control to obtain the fold change in expression post-lesion. I log transformed the fold change data to fit a Gaussian distribution for parametric statistical analysis. A One-way ANOVA and Tukey's multiple comparisons test was performed using GraphPad Prism 7 statistical software.

Solutions and Reagents

Phosphate Buffered Saline (PBS): 10 mM PO_4^{3-}, 137 mM NaCl, and 2.7 mM KCl.

Phosphate Buffer (0.2M PB): 0.2 M NaH_2PO_4 (monobasic), 0.2 M Na_2HPO_4.

Electrophoresis Buffer (TAE): 40 mM Tris base, 20 mM Acetic Acid, 1 mM Ethylenediaminetetraacetic acid (EDTA). *Tank buffer for Western blot:* 25 mM Tris base,

192 mM glycine, in 10% SDS and 20% methanol. *Blotting Buffer for Western blot:* 25 mM Tris base, 192 mM glycine, in 0.1% SDS and 20% methanol. *Tris-buffered saline (TBS):* 44.5 mM Tris HCl, 5.5 mM Tris base, 150 mM NaCl, 2.4 mM $CaCl_2$. *Anti-ADAM23:* The rabbit polyclonal antibody was affinity purified. It was splice variant non-specific, targeting a conserved region in the Disintegrin domain.

Western Blotting

The remaining aqueous phase from RNA isolation was carefully pipetted off the interphase and phenol phase which had been stored overnight at 4°C prior to adding 300 uL of 100% ethanol and mixing by inversion. The samples were allowed to set 3 min at room temp before centrifuging 2,000 g for 5 min at 4°C. Supernatants were split between two tubes (~300 µl each) before adding 3x volume of isopropanol. The tubes were mixed by inversion for 15 sec and allowed to set at room temp 10 min before centrifuging 12,000 g for 10 min at 4°C. Supernatants were discarded and 1 ml of 300 mM guanidine hydrochloride and 2.5% glycerol in 100% ethanol, a wash solution (GH), was added. The pellets were broken up manually with a syringe needle, vortexed, and allowed to incubate for 10 min at room temp before centrifuging 8,000 g for 5 min at 4°C. This wash step was repeated 2x and samples could be stored in the GH solution at -80°C and prepared further before use. A wash with 1ml 2.5% glycerol in 100% ethanol was performed then samples were vortexed, allowed to set 10 min at room temp, and centrifuged 8,000 g for 5 min at 4°C. The pellet was solubilized in 1% sodium dodecyl sulfate (SDS) in PBS with protease inhibitors: 1 µg/mL pepstatin A, 1 µg/ml leupeptin, 2 µg/mL aprotinin, 10 µg/mL phenylmethylsulfonyl fluoride, and 10 mM Na_3VO_4. For equal loading of

Western lanes a Pierce BCA protein assay kit (Thermo Fischer) was used to quantify sample protein concentrations.

Samples were heated for 5 min at 95°C, cooled on ice 1-2 min, and centrifuged before running on a 30% acrylamide gel in tank buffer for ~1 hr at 150V. Gels were soaked in blotting buffer for 15 min and transferred to nitrocellulose at 100V for 90 min. Blots were rinsed in water and incubated in 700 nm REVERT total protein stain (LI-COR) for 5 min, rinsed with REVERT wash solution, and imaged on an Odyssey FC imaging system (LI-COR). The REVERT reversal solution was applied for 5 min. Blots were then rinsed with water and washed 3 x 10 min in TBS, 3 x 10 min in TTBS, and blocked for 1 hr in 1:1 Odyssey blocking buffer (LI-COR) and TBS. The anti-ADAM23 primary anti-body was diluted 1:500 in Odyssey block:TBS with 0.2% Tween-20 and the blot was allowed to incubate overnight at 4°C. It was washed 3 x 10 min in TBS 0.2% Tween-20 (TTBS) and incubated with 800 nm donkey ant-rabbit secondary (LI-COR for 90 min at room temp. It was then washed 3 x 10 min in TTBS, 3 x 10 min in TBS, and re-imaged. The blot was blocked in 1:1 Odyssey block:TBS for 1 hr before re-probing with mouse anti-Tubulin antibody (1:2000) in 1:1 Odyssey block:TBS with 0.2% Tween-20 overnight at 4°C. Blots were washed 3 x 10 min in TTBS and incubated 90 min in 680 nm donkey anti-mouse secondary (LI-COR) 1:5000 in 1:1 Odyssey block:TBS with 0.2% Tween-20. It was again washed 3 x 10 min in TTBS, 3 x 10 min TBS, and imaged.

Western Blot Data Analysis

In Image Studio software (LI-COR) version 5.2, the Western blot analysis tools was used to measure signal strength in lanes (total protein) and bands (ADAM23, α-tubulin) by drawing rectangular shapes. The median background in the gel was

subtracted. The images were also analyzed in Image J using the gel analysis tool to select spatial peaks in density from each lane for comparison. This involved drawing lines to mark where peaks could be distinguished from background. There was a lot of background from remaining total protein stain. Relative densities were calculated for ADAM23 peaks and control peaks separately. The signal values and relative density measurements from total protein or α-tubulin controls were transformed into normalization factors (fraction of the highest value) by which ADAM23's signal was divided. This normalized signal was then transformed into a fraction of the highest value within replicates so they could be averaged despite differences in scale. The normalized values for ADAM23 were compared across saline and lesion conditions and across days post-injection by performing a 2-Way ANOVA and Tukeys multiple comparison test in GraphPad Prism 7 statistical software.

CHAPTER THREE

RESULTS

In Silico Identification of Candidate Genes Involved in Regeneration

I was initially interested in identifying genes that regulate neurogenesis and the regenerative capacity of NPCs in the OE. Therefore, I examined data from three separate microarray studies in the GEO database (Heron et al, 2013; Shetty et al, 2005; Borders et al, 2007) to identify genes expressed in the OE that are significantly different following injury. In these studies, OSN cell death and subsequent regeneration was induced by olfactory bulbectomy, a well characterized surgical method of OE lesion. I looked for altered gene expression (common to all three studies) using GEO2R, an online tool which analyzes differences between user-selected groups (control, days post-injury) with correction for multiple-tests. Several *Adams* exhibited a change in expression early post-injury, within one to five days. *Adam23* in particular decreased in expression in all three microarray studies (adj. pval<0.05), as early as day two. In one study, *Adam22* decreased in expression by day five (adj. pval<0.05), while in another *Adam4* and *Adam10* increased in expression by day two (adj. pval<0.05). I reviewed the current literature and determined if any of the gene candidates had the appropriate structure for signal transduction, were known to have interaction partners in the OE, were critical for nervous system development, or were implicated in stem cell regulation in other tissues (Carter et al, 2004, Mitchell et al, 2001, Sun et al, 2007; Wang et al, 2012). I identified *Adam23* as the most promising of the gene candidates because of its involvement (along

with other *Adam* family members) in cell-cycle regulation (Verbisck et al, 2009, Kang et al, 2000; Kang et al, 2001, Sun et al, 2010).

Adams are Expressed in the Olfactory Epithelium

After, having selected *Adam23* for further study, I designed primers for both its known and predicted splice variants along with primers for additional *Adam* family members (Table 1). After isolating mRNA from olfactory epithelia and transcribing cDNA from these transcripts, I used RT-PCR to detect the presence or absence of transcript in OE tissue. I found that four *Adam23* splice variants are expressed in OE tissue as well as transcripts for *Adam4*, *Adam21*, and *Adam10* (Figure 3). I then focused my efforts on *Adam23* due to the agreement between microarray studies and the results of the literature search.

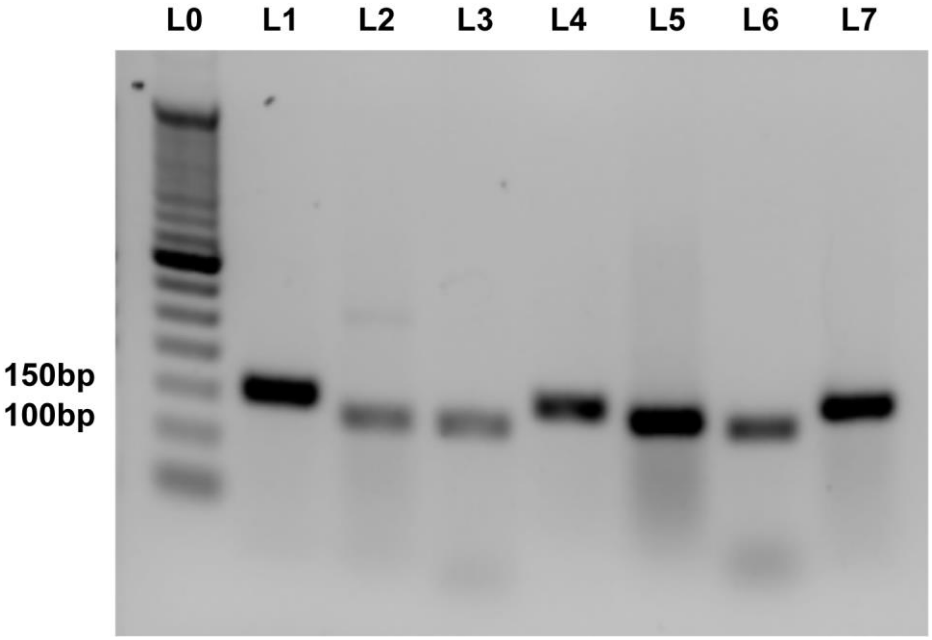

Figure 3. *Adams* Expressed in the Olfactory Epithelium. cDNA generated from RT-PCR of extracted RNA. Gel electrophoresis of PCR products. (L0) 50 bp ladder, (L1) *Adam23v2*, (L2) *Adam23x1*, (L3) *Adam23x2*, (L4) *Adam23v1*, (L5) *Adam4*, (L6) *Adam21*, (L7) *Adam10*.

As I had evidence that *Adam23* transcripts were present in the OE, my next goal was to identify whether ADAM23 protein was detected in the OE. To this end, I used immunohistochemistry (IHC) to verify the presence of ADAM23 protein and its cellular localization in normal OE tissue which had been perfused and cryosectioned (Figure 4). Because there is evidence that different portions of the OE express different classes of odorant receptors (Bozza et al, 2009), different cell adhesion molecules (Yoshihara et al, 1997), and therefore ADAM expression may not be uniform throughout, I compared expression in the dorsal recess and dorsal septum, also known as "Zone 1", versus the ventral septum and nasal turbinates, generally referred to as "Zones 2-4" (Figure 1B). In the dorsal recess and along parts of the septum, ADAM23 expression was detected primarily in Sus cell bodies and in their processes extending down to the basal OE (Figure 4 A-H). Labeling in basal cells of the OE was inconsistent but coincided with zones of Sus labeling. For some turbinates, ADAM23 labeling was also found in neurons (Figure 4 I-P). Much of the protein detected appeared to be cytosolic in Sus cells and sometimes nuclear in neurons.

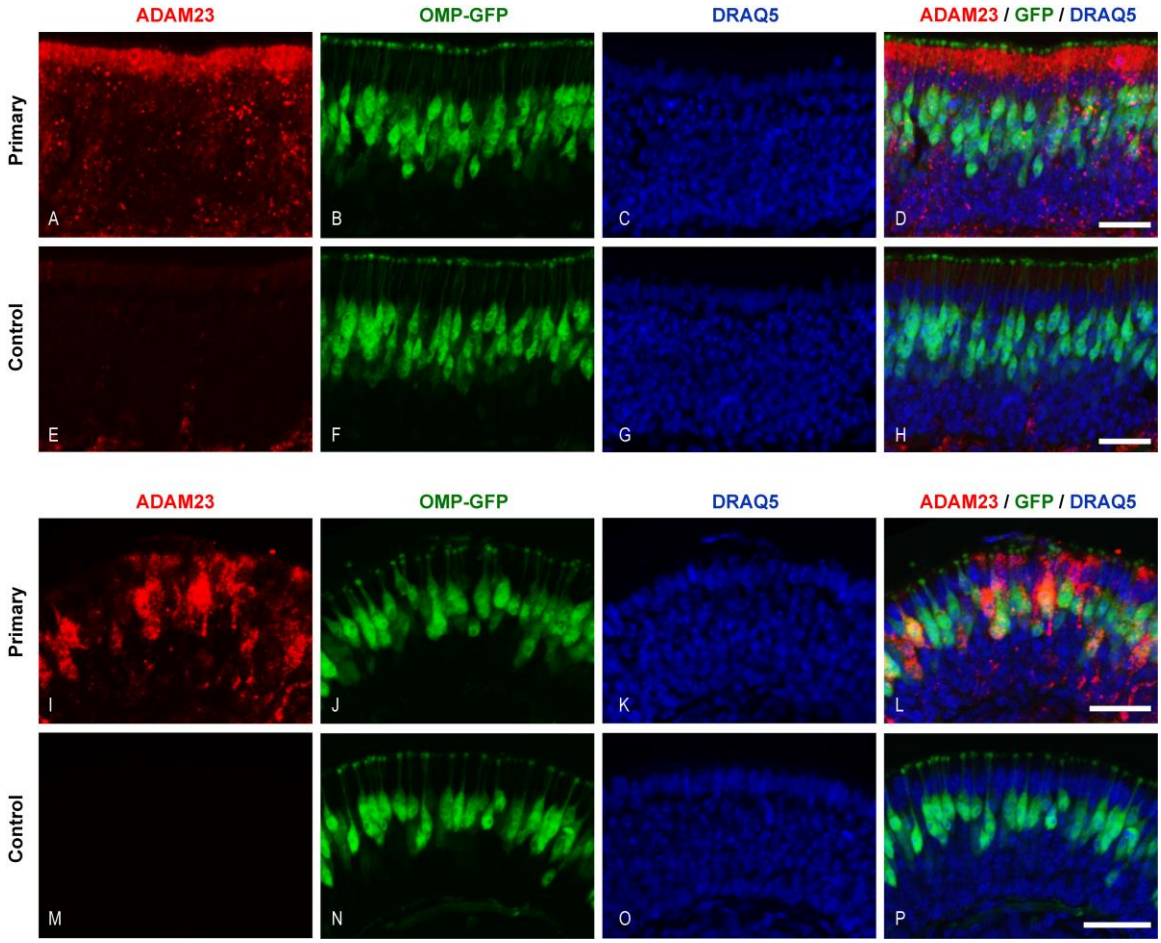

Figure 4. ADAM23 Expression in the Olfactory Epithelium. Immunofluorescence labeling of ADAM23 (red) in OMP-GFP transgenic mouse OE (green, mature neurons) with DRAQ5 (blue, nuclei marker), p15. Scale bar 25 µm. (A-D) ADAM23 localized in Sus cell bodies and processes along the septum near the dorsal recess. (E-H) Omission of anti-ADAM23 primary (control), view of septum near the dorsal recess. (I-L) ADAM23 localization in neurons of turbinate. (M-P) Omission of anti-ADAM23 primary (control), view of turbinate.

ADAM23 Co-localization with Sus and Neuron Markers

Once I had evidence that ADAM23 protein is expressed in the OE, I next turned to confirming the cell type(s) that it is localized in. ADAM23 was co-localized with the Sus cell marker ECAD in the dorsal recess (Figure 5 A-H). When antigen retrieval was performed, ADAM23 still appeared primarily in Sus cells, though the processes were no longer visible and contact with the ICAM labeled HBCs was obscured (Figure 5 I-P). In

the turbinates, ADAM23 protein expression was detected in both immature neurons identified by their DCX expression, and in mature neurons identified by GFP expression in the OMP-GFP transgenic reporter mouse (Figure 6 A-P). To quantify the percent of OE cells which are ADAM23 positive, and of those how many are neurons, I performed ICC on dissociated cells from OE tissue. Nearly all of the cells labeled for ADAM23 were also positive for a nuclear marker (90.4 ± 0.079 %, n=4; Figure 7). There were 1.74x more ADAM23 positive cells in cultures exposed to both the rabbit anti-ADAM23 antibody and a secondary antibody versus those for which the primary antibody was omitted as a control ($p<0.05$, $n = 4$). However, in cells dissociated from the OEs of OMP-GFP reporter mice, I did not detect any difference (0.99x) between the number of cells co-labeled with both ADAM23 and GFP in anti-ADAM23 treated cultures versus controls (n=4).

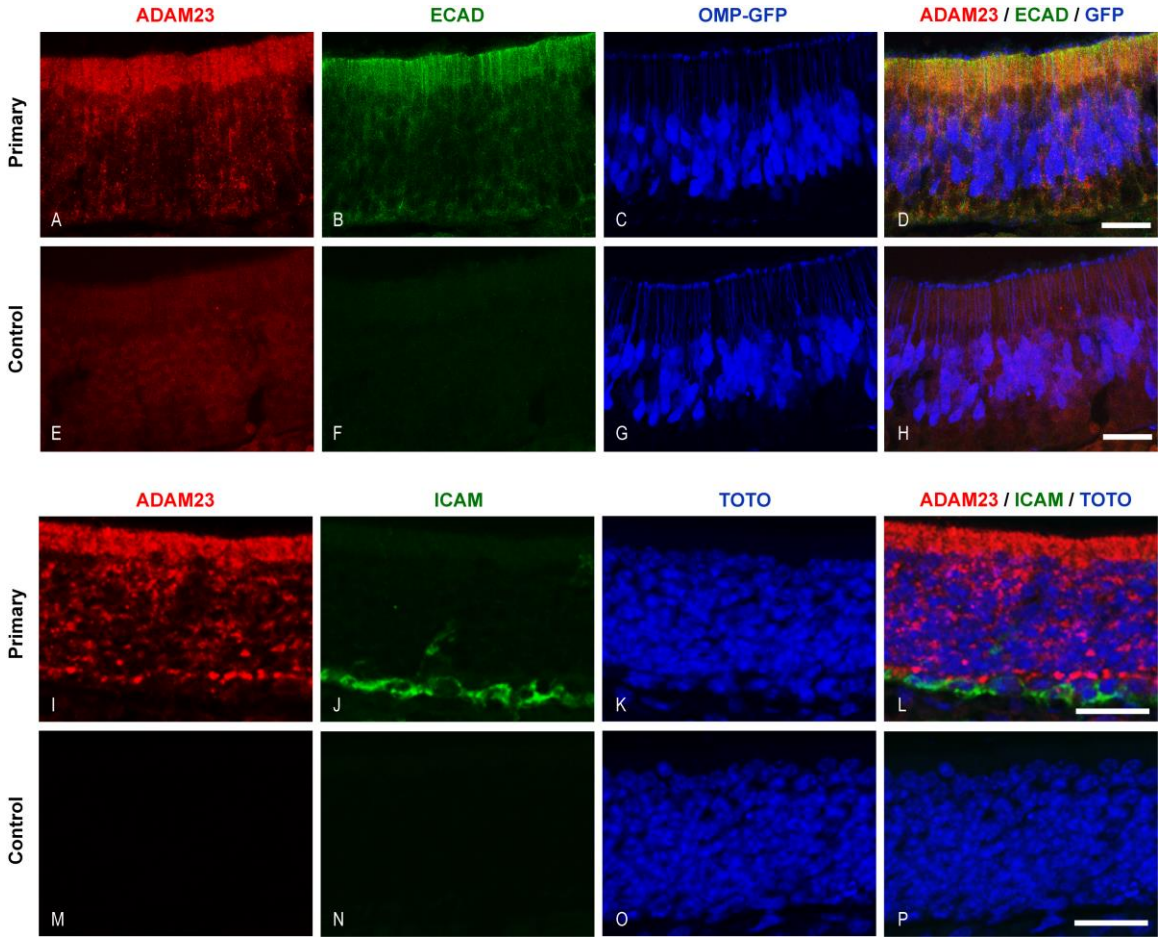

Figure 5. ADAM23 Expression in Sus with Projections to HBCs. Co-localization of ADAM23 (red) with Sus and HBC markers. Scale bars 25 µm. (A-D) ECAD (green, Sus) in dorsal recess of OMP-GFP mouse OE (blue, mature neuron), p20. (E-H) Comparison to omission of anti-ADAM23 and anti-ECAD primaries (control), view of dorsal recess. (I-L) ICAM (green, HBC) with TOTO (blue, nuclei) in septum near dorsal recess after antigen retrieval, p81. (M-P) Comparison to omission of anti-ADAM23 and anti-ICAM primaries (control), view of septum.

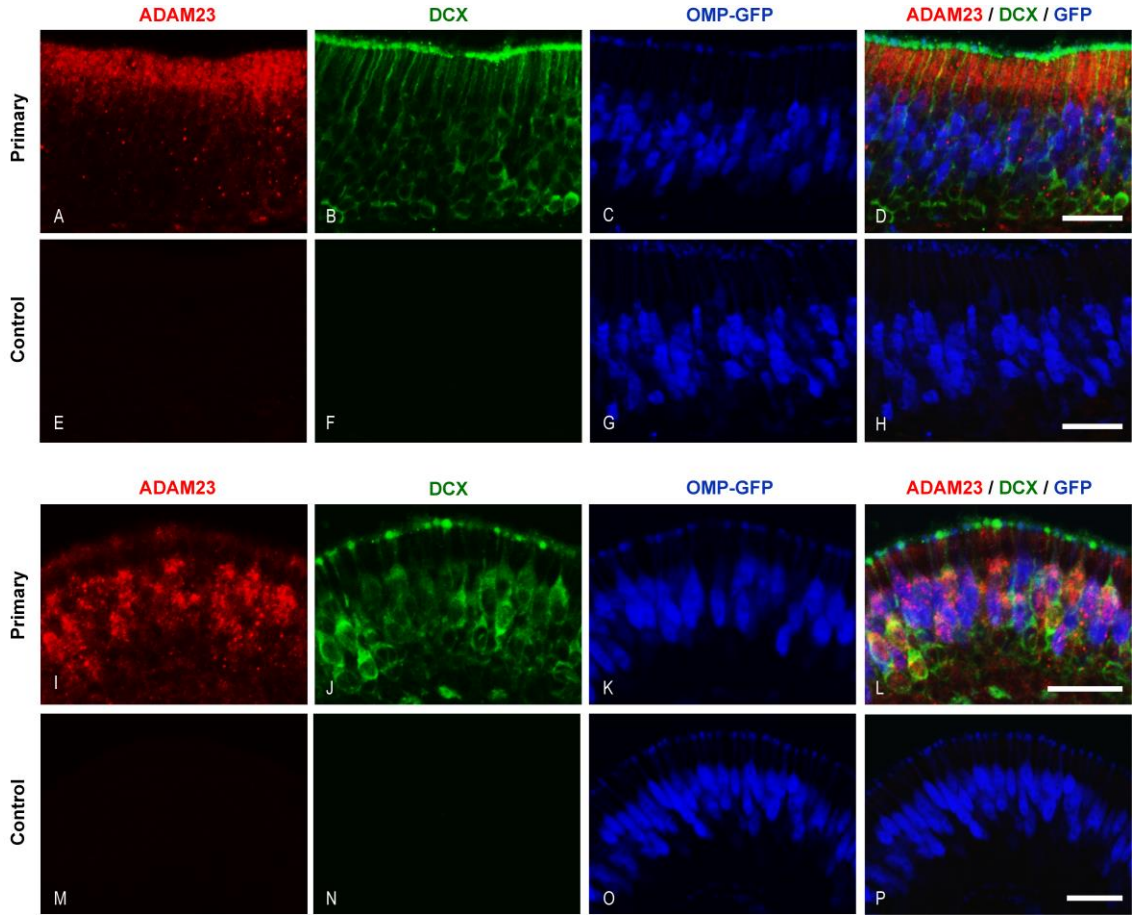

Figure 6. ADAM23 Expression in Neurons. Co-localization of ADAM23 (red) with mature and immature neuron markers. Scale bars 25 µm. (A-D) DCX (green, immature neuron) in dorsal recess of OMP-GFP mouse OE (blue, mature neuron), p19. (E-H) Comparison to omission of anti-ADAM23 and anti-DCX primaries (control), view of dorsal recess. (I-L) DCX (green, immature neuron) in turbinate of OMP-GFP mouse OE (blue, mature neuron), p19. (M-P) Comparison to omission of anti-ADAM23 and anti-DCX primaries (control), view of turbinate.

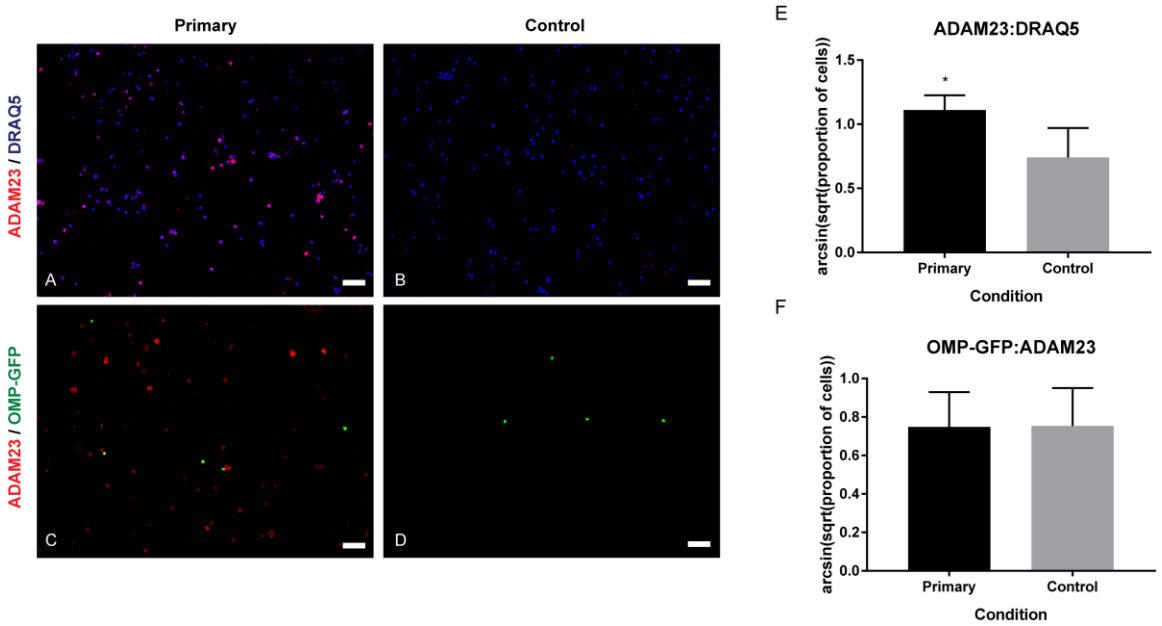

Figure 7. Proportion of OE Cells that Express ADAM23. Cells were dissociated with papain and plated. Comparison to omission of primary control. Scale bars 50 µm. (A) ADAM23 (red) with DRAQ5 (blue, nuclei). (B) Omission of anti-ADAM23 primary (red) with DRAQ5 (blue). (C) ADAM23 (red) with OMP-GFP (green, mature neurons). (D) Omission of anti-ADAM23 primary (red) with OMP-GFP (green). (E) Proportion of DRAQ5 positive cells also ADAM23 positive, arcsinsqrt transformed. Comparison between primary and omission of primary control. (F) Proportion of ADAM23 positive cells also positive for OMP-GFP, arcsinsqrt transformed. Comparison between primary and omission of primary control with t-test, n=4 *p<0.05.

ADAM23 Expression Changes During Postnatal Development

While examining ADAM23's expression in OE, I did not detect ADAM23 protein in tissue from mice of age p3-4 as compared to tissue from mice age p15 and older (Figure 8). *Adam23*'s expression during post-natal development is relevant to understanding its role in the OE. To this end I determined relative transcript expression using RT-qPCR (same primers, Table 1) after extracting mRNA from tissue at age p1, p5, p10, p15, p20, p30, p60, p120, and 12 months. The three *Adam23* splice variants examined increase in expression between p1 and p15 (n=1). Expression of *Adam23v2* and *Adam23x2* increases through at least p120 (fold change = 7.49 and 2.37, respectively) and

likely asymptotes thereafter, whereas *Adam23x1* expression peaks earlier at p10 (fold change = 2.80).

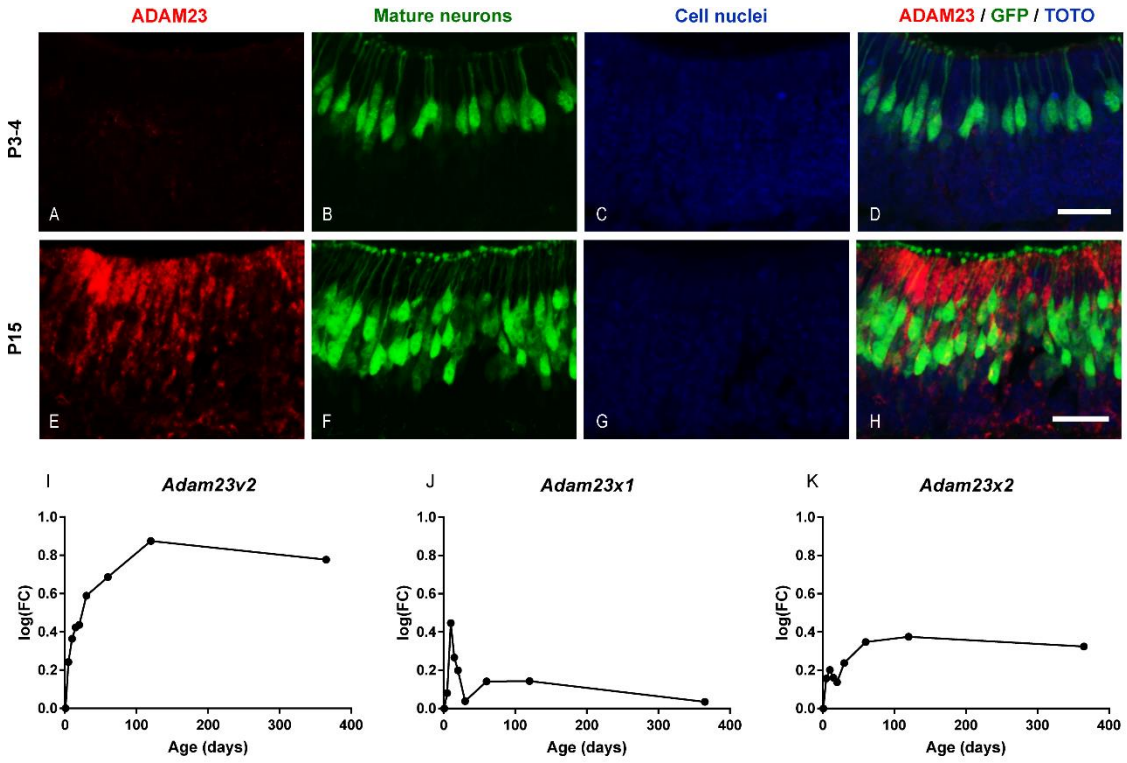

Figure 8. ADAM23 Expression Changes During Postnatal Development. Comparison of ADAM23 expression between age p3-4 and p15. Scale bars 25 µm. (A-D) ADAM23 (red) with OMP-GFP (green, mature neurons) and TOTO (blue, nuclei) in dorsal recess, p3-4. (E-H) ADAM23 (red) with OMP-GFP (green, mature neurons) and TOTO (blue, nuclei) in dorsal recess, p15. (I) RT-qPCR log(fold change) *Adam23v2* expression increases during post-natal development (n=1). (J) RT-qPCR log(fold change) *Adam23x1* expression peaks at p10 during postnatal development (n=1). (K) RT-qPCR log(fold change) *Adam23x2* expression increases during postnatal development (n=1).

Adam23 Gene Expression is Altered as the OE Regenerates

After verifying the expression of *Adam23* and its protein product in intact OE tissue, I performed RT-qPCR on tissue collected 1, 3, 5, 7-8, and 12-14 days post-methimazole lesion, to determine whether *Adam23* is differentially expressed during lesion recovery and how its pattern of expression compares to that of cell specific markers (Figure 9). All four *Adam23* splice variants decreased in expression days 1-8

post-lesion before returning to control levels (log(FC) = -0.74, -0.69, -0.42, and -0.61). The decrease from control was not as dramatic as the decrease in the OSN_m marker (log(FC) = -1.35). The HBC marker, *ΔNp63*, increased in expression by day 3 post-lesion (log(FC) = 0.55). The GBC marker, *Ascl1*, increased in expression with peak at day 5 post-lesion (log(FC) = 0.65). The Sus cell marker, *Ecad*, increased in expression by day 3 post-lesion (log(FC) = 0.24). The cell marker for OSN_i, *Gap43*, decreased in expression days 1-5 post-lesion, before increasing days 7-12 (log(FC) = -0.60). The OSN_m cell marker, *OMP*, decreased in expression days 1-7 post-lesion, before increasing by day 12 post-lesion.

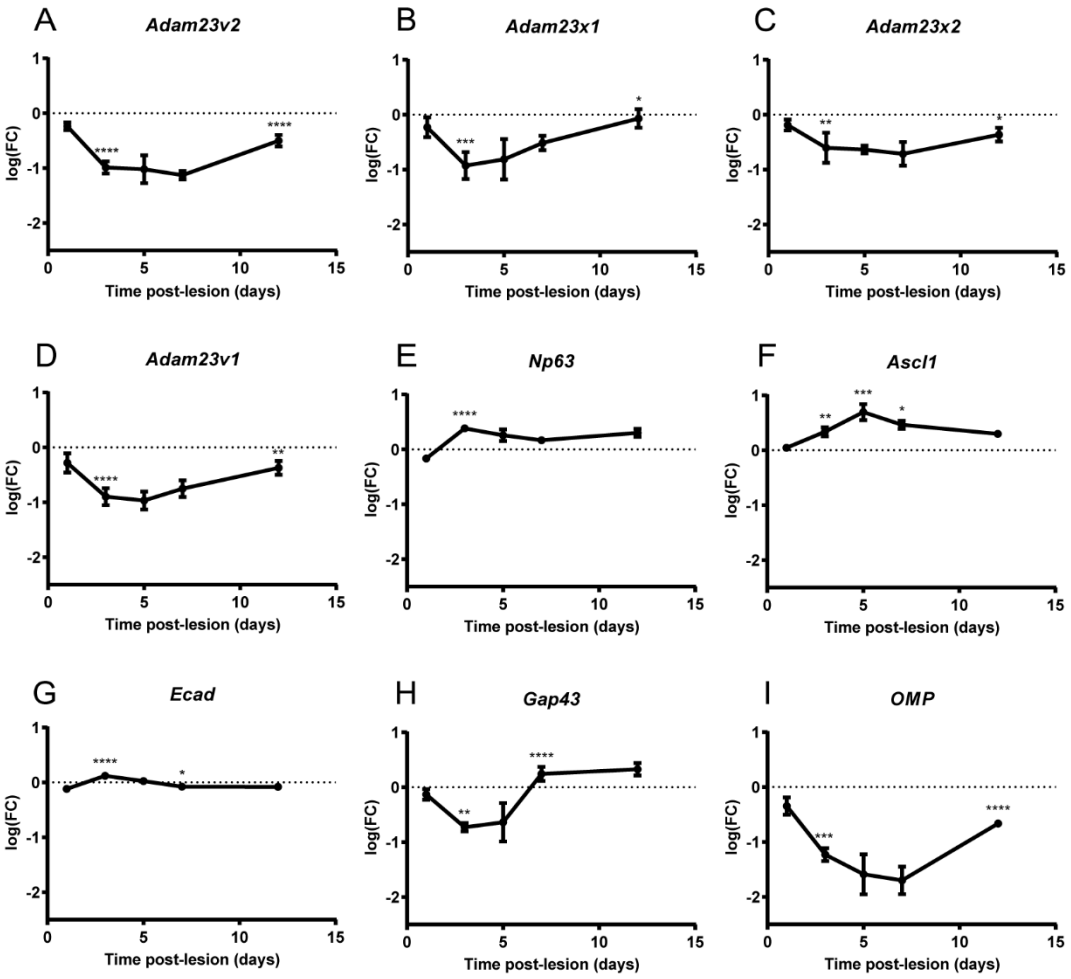

Figure 9. *Adam23* Gene Expression is Altered Post-Lesion. Log transformed fold change in *Adam23* splice variant and cell marker expression, as measured by RT-qPCR for days 1, 3, 5, 7-8, and 12-14 post-lesion, compared to saline controls. Expression was calculated using the $2^{\wedge-\Delta\Delta CT}$ method with *Pgk1* and *Tfrc* for reference genes. One-way ANOVA's were performed followed by Tukey's multiple comparison test. Asterisks are used to denote significant differences between a point and the point immediately preceding it (*p<0.05, **p<0.01, ***p<0.001, ****p<0.0001). (A)(B)(C)(D) Adam23 splice variants decrease in expression days 1-8 post-lesion before returning to control levels, n=6. (E) ΔNp63, an HBC cell marker, increases in expression by day 3 post-lesion, n=4. (F) Ascl1, a GBC cell marker, increases in expression, with peak at day 5 post-lesion, n=4. (G) Ecad, a Sus cell marker, increases in expression by day 3 post-lesion, n=2. (H) Gap43, an OSN_i cell marker, decreases in expression days 1-5 post-lesion, before increasing days 7-12 post-lesion, n=4. (I) OMP, an OSN_m cell marker, decreases in expression days 1-7 post-lesion, before increasing by day 12 post-lesion, n=4.

ADAM23 Protein Levels are Altered as the OE Regenerates

Next, I wanted to determine whether the changes observed in *Adam23* mRNA expression are reflected in ADAM23 protein levels post-lesion. Protein was isolated from the same OE tissue samples that were used for RT-qPCR. The ADAM23 antibody used in IHC also recognized a band corresponding to the expected molecular weight (Mr = 90 kDa) of ADAM23 in its preprotein form (Figure 10). In lanes for lesion day (L1), (L3), and (L5) another band is faintly seen which is likely the cleaved form of the protein (Mr = 71 kDa). Two methods of normalization were used. First, blots were exposed to a total protein stain prior to antibody incubations. However, the total protein stain was not completely reversible. Second, blots were probed with an antibody detecting tubulin after ADAM23 antisera incubation. The protein stain provides evidence for equal loading between lanes whereas α-tubulin and ADAM23 both change in expression level in alternating lanes. Normalizing to one versus the other yields opposite results. When normalizing to α-tubulin in Image J, ADAM23 protein levels are not different between lesion and saline conditions (FC = 0.83, 0.44, 0.45, 0.08, 0.40, days 1-12 respectively; n=4, 2-way ANOVA). When normalizing to total protein in either Image J or Image Studio, ADAM23 protein is significantly upregulated between lesion and saline control day 3 (FC = 2.43, $p<0.05$, n=4, 2-way ANOVA).

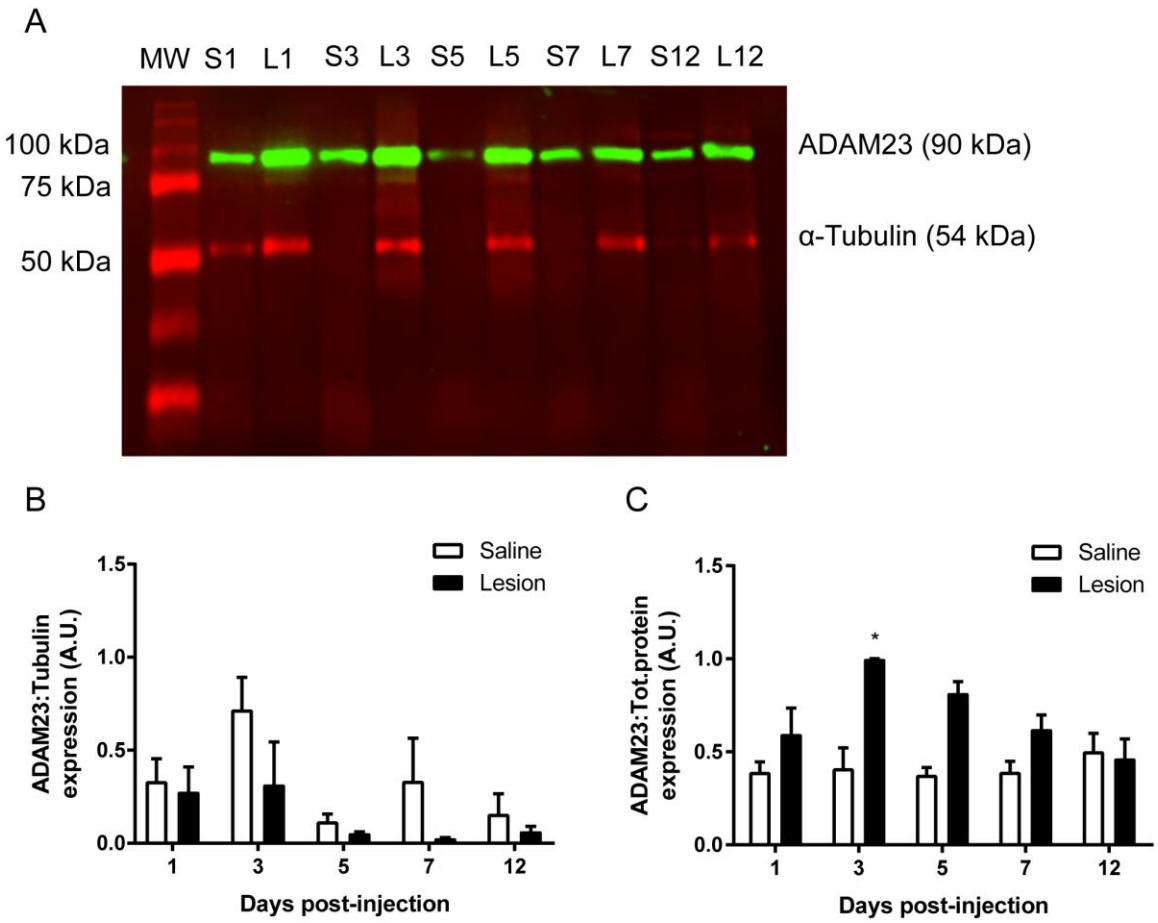

Figure 10. ADAM23 Protein Expression is Altered Post-Lesion. (A) Western blot showing ADAM23 (green, expected Mr = 70/90 kDa) and α-Tubulin (red, expected Mr = 54 kDa) after total protein stain reversal. L0: Molecular weight marker (MW), S1: saline day 1, L1: lesion day 1, S3: saline day 3, L3: lesion day3, S5: saline day 5, L5: lesion day 5, S7: saline day 7-8, L7: lesion day 7-8, S12: saline day 12-14, L12: lesion day 12-14. (B) ADAM23 protein expression in lesion and saline controls, normalized to α-Tubulin. Two-way ANOVA showed no significant differences between saline and lesion conditions or between days post injection ($n=4$, $p>0.05$). (C) ADAM23 protein expression in lesion and saline controls, normalized to total protein. Two-way ANOVA showed significant differences between saline and lesion conditions and between days post injection ($n=4$, $p<0.01$, $p<0.05$). Tukey's multiple comparison test found a significant increase between day 1 and day 3 post-lesion (* $p<0.05$).

CHAPTER FOUR

DISCUSSION

My goal was to identify genes of importance in the OE for maintaining and activating the resident NPC populations. I hypothesized that such genes would be involved in cell signaling, signal transduction, and tie into pathways regulating the cell cycle in NPCs. I also expected such genes would be dynamically regulated during regeneration. The ADAMs are a family of proteins involved in these processes that I identified by examining published microarray expression data post-bulbectomy (Heron et al, 2013; Shetty et al, 2005; Borders et al, 2007). *Adam23* expression in particular decreased in all three microarrays and is implicated in stem cell regulation (Sun et al, 2007; Wang et al, 2012). First, I confirmed *Adam23* expression in the OE, and observed that multiple splice variants were present. I then identified what cell types express ADAM23 protein, and finally I measured changes in mRNA and protein expression during times of cell death, proliferation, and regeneration.

Multiple cell types express ADAM23 protein as labeled with IHC. ADAM23 is in both Sus cell bodies and along their basal processes. Interestingly, the contact of HBCs with Sus end-feet via primary cilia regulates regeneration in the OE (Joiner et al, 2015). Indeed, it has also been shown that Sus can induce basal cell proliferation via purine signaling (Hassenklover et al, 2008). It may be that the ADAM23:integrin interaction is disrupted during injury to sensitize NPC's to other signals for repair in their environment.

ADAM's interaction partners, the integrins, have not been fully characterized in the OE. A previous study demonstrated strong integrin labeling on the basal surface of HBCs (Carter et al, 2004). However, while the authors did not emphasize it, I also observed integrin immunoreactivity in Sus cell bodies. This provides support for a possible interaction between the ADAMs observed in mature neurons and integrin-expressing Sus cells. Disruption of Neuron:Sus contact upon neuron death may activate signaling in Sus cell bodies traveling apical to basal (Miragall et al, 2004; Makino et al, 2009).

I did not observe Sus or neuron labeling in tissue sections from very young mice age p3-4. My preliminary RT-qPCR data is in agreement with my hypothesis that *Adam23* is developmentally regulated, increasing in expression between p1 and p15. The RT-qPCR results for the splice variant *Adam23x2* (*gamma*) did not follow the general pattern observed in a previous study with tissue from whole mouse brains. In that study, a variant named *gamma*, lacking a transmembrane domain, was expressed embryonically but was down-regulated by p10, while variants *alpha* and *beta*, differing in composition by 91 base pairs in the transmembrane region, were expressed into adulthood (Sun et al, 2004).

The sequences of these three variants correspond to reference sequences in the NCBI database named *Adam23-variant2* (*v2, beta*), *Adam23-predicted-variant1* (*x1, alpha*), and *Adam23-predicted-variant2* (*x2, gamma*). These three were expressed in OE tissue along with *Adam23-variant1* (*v1*). The *Adam23-predicted-variant3* (*x3*) was not expressed. Both *Adam23v1* and *Adam23x3* have recently been removed from the database due to lack of experimental evidence. *Adam23v1* is present in OE tissue, but whether it is

processed into protein remains an open question. It may, like *Adam23x2* (*gamma*), be a soluble isoform secreted by the cell or cytosolic and compete with binding of ADAM23 extracellularly and/or intracellularly.

I observed that *Adam23* expression decreased post-methimazole lesion, in agreement with the microarray studies post-bulbectomy. Even with this higher resolution look at the recovery time-series, days 1, 3, 5, 7-8, and 12-14 post-lesion, changes in expression cannot be tied to regulation in any one cell-type. By examining the expression of cell-specific markers the death and regeneration of OE cell-types can be marked. The overall decrease of *Adam23* in OE tissue due to the death of neurons may mask any down- or up-regulation in surviving Sus and NPCs. It was unexpected that Sus cell marker *Ecad* should increase post-lesion, indicating that methimazole lesion may not cause much Sus cell death and Sus cells may proliferate immediately following lesion. The increase in HBC marker *ΔNp63* by 3 days post-lesion, followed by a peak in GBC marker Ascl1 5 days post-lesion, and subsequent increases in *Gap43* and *Omp*, recapitulates the timing of proliferation and recovery observed in previous Brdu experiments. This is the only study to use RT-qPCR and not microarray to observe changes in cell marker expression post-lesion. Our results agree with the microarray findings. Small changes in expression were more easily detected and replicated. The only other study which used RT-qPCR in the OE was limited to gene expression in FACS sorted HBCs (Fletcher et al, 2011).

Finally, I did not observe a corresponding decrease in ADAM23 protein levels post-lesion, as quantified in Western blot by normalization to α-tubulin. While the difference between the saline and lesion condition was not significant ($n=4$, $p>0.05$) due

to high variation, this could be resolved with a greater number of replicates. The absence of ADAM23 mediated cell-signaling post-lesion could in some way induce the repair response in the OE. Alternately, when normalized to total protein ADAM23 increases significantly ($n=4$, $p<0.05$) in conflict with the RT-qPCR data. This would mean that some other form of regulating the protein exists and that it is likely important for mediating cell-cell interactions during recovery of the stratified epithelium.

This work provides a basis for further study of ADAM23. I show evidence that it is expressed in the OE as both transcript and protein. That it has multiple splice variants and may be expressed in both Sus and neurons in a region dependent manner. I show that *Adam23* mRNA expression decreases post-lesion in a pattern similar to expression of the mature neuron marker OMP. This information and the preliminary protein expression data will allow for an educated hypothesis about ADAM23's functional importance in the OE and will guide the design of future experiments. Through study of ADAM23, the field of neural regeneration could gain a better understanding of the importance of Sus:NPC and Sus:neuron interactions in tissue repair. The cellular processes which can be regulated by a catalytically inactive member of the ADAM family through interaction with integrins is also of interest and could provide a missing link in the NPC activation cascade.

CHAPTER FIVE

FUTURE DIRECTIONS

From the evidence I have accumulated so far ADAM23 likely mediates signaling between Sus and NPCs and between Sus and neurons. Sus have not received much attention in the regenerating OE until recently. We know that Sus cell morphology changes post-injury (Makino et al, 2009), and contact between the primary cilia of NPCs and Sus cell end-feet is important for neurogenesis during post-natal development and during regeneration (Joiner et al, 2015). Characterizing the signaling mechanisms behind these cellular responses would be of significance in understanding why neural regeneration is supported throughout life in the OE.

Before investigating the functional importance of ADAM23 in the OE, the localization of ADAM23 protein and its expression by Sus and neurons must be further supported. Localization to a particular cell-type has relied on the specificity of an antibody (SC50482, Santa Cruz). Immunogen pre-adsorption was not performed as a control since the immunizing peptide was not commercially available; however, we may be able to synthesize the peptide to perform these controls. The antibody could also be used for IHC on the ADAM23 knockout mouse (B6:129S5-Adam23^{tm1Lex}) as another control for specificity. Tissue from a reporter mouse could be used to determine cellular expression (Tg(Adam23-EGFP)LR169Gsat/Mmucd). In addition to these methods, an *in situ* hybridization could be performed to examine mRNA expression and localization.

In addition, IHC in saline and lesion condition tissue would be of interest to

to confirm the RT-qPCR expression findings. Reduced labeling of ADAM23 in Sus post-lesion may coincide with markers of proliferation in the Sus themselves or in the NPCs. To support these results quantification of protein levels should be completed with equal loading and a reliable method of normalization. The RT-qPCR expression of Adam23 during post-natal development should also be completed and compared to the onset of cell specific markers. An increase in *Adam23* expression by p15 should coincide with a decline in proliferation and upregulation of genes such as *ΔNp63* known to control the reserve status of HBCs.

Co-localization of ADAM23 with Sus and neuron cell markers was observed in OE tissue. Further IHC could be performed showing co-localization with integrins or with LGI proteins. Immunoprecipitation could be used to identify ADAM23's interaction partners. OE NPCs could be cultured and the ability to form neurospheres measured after application of ADAM23's disintegrin domain, which could be used to either block the ADAM23 signal transduction cascade leading to increased differentiation or to activate its binding partners and promote self-renewal.

Finally, to get at a function for ADAM23 *in vivo* a conditional knockout mouse (C57BL/6N-Adam23$^{tm1a(EUCOMM)Hmgu/H}$) could be ordered, or knockout of ADAM23 in Sus cells, could be done using RNA interference or CRISPR/Cas9. The structure of the OE would be examined histologically for changes in the cell layers, in cell morphology, for displaced cells, and for increased or decreased OE thickness. The ability to recover from lesion may be impaired taking a longer time for recovery.

A strong case could be made, having established expression, localization, interaction, and a conditional knockout phenotype, that ADAM23 is necessary for

regeneration. ADAM23 may demonstrate further the importance of Sus cell interactions in maintaining and activating the NPC populations of the OE. Our strategy to identify a gene of interest for maintaining NPC quiescence has turned up an otherwise overlooked candidate for further study.

BIBLIOGRAPHY

Andersen CL, Jensen JL, Ørntoft TF. (2004). Normalization of real-time quantitative reverse transcription-PCR data: a model-based variance estimation approach to identify genes suited for normalization, applied to bladder and colon cancer data sets. Cancer Res. 64(15):5245-50.

Barry DS, Pakan JM, McDermott KW. (2014). Radial glial cells: key organisers in CNS development. Int J Biochem Cell Biol. 46:76-9.

Böhm BB, Freund I, Krause K, Kinne RW, Burkhardt H. (2013). ADAM15 adds to apoptosis resistance of synovial fibroblasts by modulating focal adhesion kinase signaling. Arthritis Rheum. 65(11):2826-34.

Borders AS, Hersh MA, Getchell ML, van Rooijen N, Cohen DA, Stromburg AJ, Getchell TV. (2007). Macrophage-mediated neuroprotection and neurogenesis in the olfactory epithelium. Physiol Genomics. 31(3):531-43.

Bozkulak EC, Weinmaster G. (2009). Selective use of ADAM10 and ADAM17 in activation of Notch1 signaling. Mol Cell Biol. 29(21):5679-95.

Bozza T, Vassalli A, Fuss S, Zhang JJ, Weiland B, Pacifico R, Feinstein P, Mombaerts P. (2009). Mapping of class I and class II odorant receptors to glomerular domains by two distinct types of olfactory sensory neurons in the mouse. Neuron. 61(2):220-33.

Brann JH, Firestein SJ. (2014). A lifetime of neurogenesis in the olfactory system. Front Neurosci. 8:182.

Brann JH, Ellis DP, Ku BS, Spinazzi EF, Firestein S. (2015). Injury in aged animals robustly activates quiescent olfactory neural stem cells. Front Neurosci. 9:367.

Bridges LC, Lingo JD, Grandon RA, Kelley MD. (2008). All-trans-retinoic acid induces integrin-independent B-cell adhesion to ADAM disintegrin domains. Biochemistry. 47(15):4544-51.

Cal S, Freije JM, López JM, Takada Y, López-Otín C. (2000). ADAM 23/MDC3, a human disintegrin that promotes cell adhesion via interaction with the alphavbeta3 integrin through an RGD-independent mechanism. Mol Biol Cell. 11(4):1457-69

Carter LA, MacDonald JL, Roskams AJ. (2004). Olfactory horizontal basal cells demonstrate a conserved multipotent progenitor phenotype. J Neurosci. 24(25):5670-83.

Choi I, Oh J, Cho BN, Ahnn J, Jung YK, Han Kim D, Cho C. (2004). Characterization and comparative genomic analysis of intronless Adams with testicular gene expression. Genomics. 2004 Apr;83(4):636-46.

D'Abaco GM, Ng K, Paradiso L, Godde NJ, Kaye A, Novak U. (2006). ADAM22, expressed in normal brain but not in high-grade gliomas, inhibits cellular proliferation via the disintegrin domain. Neurosurgery. 58(1):179-86.

Edgar R, Domrachev M, Lash AE. (2002). Gene Expression Omnibus: NCBI gene expression and hybridization array data repository. Nucleic Acids Res. 30(1):207-10.

Fletcher RB, Prasol MS, Estrada J, Baudhuin A, Vranizan K, Choi YG, Ngai J. (2011). p63 regulates olfactory stem cell self-renewal and differentiation. Neuron. 72(5):748-59.

Fried D, Böhm BB, Krause K, Burkhardt H. (2012). ADAM15 protein amplifies focal adhesion kinase phosphorylation under genotoxic stress conditions. J Biol Chem. 287(25):21214-23.

Gaultier A, Cousin H, Darribère T, Alfandari D. (2002). ADAM13 disintegrin and cysteine-rich domains bind to the second heparin-binding domain of fibronectin. J Biol Chem. 277(26):23336-44.

Gene Ontology (GO), Mouse Genome Informatics Web Site, The Jackson Laboratory, Bar Harbor, Maine. World Wide Web (http://www.informatics.jax.org/gotools/MGI_GO_Slim_Chart.html). [August 2015].

Getchell ML, Li H, Vaishnav RA, Borders AS, Witta J, Subhedar N, de Villiers W, Stromberg AJ, Getchell TV. (2006). Temporal gene expression profiles of target-ablated olfactory epithelium in mice with disrupted expression of scavenger receptor A: impact on macrophages. Physiol Genomics. 27(3):245-63.

Hassenklöver T, Kurtanska S, Bartoszek I, Junek S, Schild D, Manzini I. (2008). Nucleotide-induced Ca2+ signaling in sustentacular supporting cells of the olfactory epithelium. Glia. 56(15):1614-24.

Heron PM, Stromberg AJ, Breheny P, McClintock TS. (2013). Molecular events in the cell types of the olfactory epithelium during adult neurogenesis. Mol Brain. 22;6:49.

Hikita A, Tanaka N, Yamane S, Ikeda Y, Furukawa H, Tohma S, Suzuki R, Tanaka S, Mitomi H, Fukui N. (2009). Involvement of a disintegrin and metalloproteinase 10 and 17 in shedding of tumor necrosis factor-alpha. Biochem Cell Biol. 7(4):581-93.

Huang X, Huang P, Robinson MK, Stern MJ, Jin Y. (2003). UNC-71, a disintegrin and metalloprotease (ADAM) protein, regulates motor axon guidance and sex myoblast migration in C. elegans. Development. 130(14):3147-61.

Iba K, Albrechtsen R, Gilpin B, Fröhlich C, Loechel F, Zolkiewska A, Ishiguro K, Kojima T, Liu W, Langford JK, Sanderson RD, Brakebusch C, Fässler R, Wewer UM. (2000). The cysteine-rich domain of human ADAM 12 supports cell adhesion through syndecans and triggers signaling events that lead to beta1 integrin-dependent cell spreading. J Cell Biol. 149(5):1143-56.

Iwai N, Zhou Z, Roop DR, Behringer RR. (2008). Horizontal basal cells are multipotent progenitors in normal and injured adult olfactory epithelium.Stem Cells. 26(5):1298-306.

Jang W, Chen X, Flis D, Harris M, Schwob JE. (2014). Label-retaining, quiescent globose basal cells are found in the olfactory epithelium. J Comp Neurol. 522(4):731-49.

Joiner AM, Green WW, McIntyre JC, Allen BL, Schwob JE, Martens JR. (2015). Primary Cilia on Horizontal Basal Cells Regulate Regeneration of the Olfactory Epithelium. J Neurosci. 35(40):13761-72.

Kamiguti AS, Zuzel M, Theakston RD. (1998). Snake venom metalloproteinases and disintegrins: interactions with cells. Braz J Med Biol Res. 31(7):853-62.

Kang Q, Cao Y, Zolkiewska A. (2000). Metalloprotease-disintegrin ADAM 12 binds to the SH3 domain of Src and activates Src tyrosine kinase in C2C12 cells. Biochem J. 352 Pt 3:883-92.

Kang Q, Cao Y, Zolkiewska A. (2001). Direct interaction between the cytoplasmic tail of ADAM 12 and the Src homology 3 domain of p85alpha activates phosphatidylinositol 3-kinase in C2C12 cells. J Biol Chem. 276(27):24466-72.

Kawaguchi N, Sundberg C, Kveiborg M, Moghadaszadeh B, Asmar M, Dietrich N, Thodeti CK, Nielsen FC, Möller P, Mercurio AM, Albrechtsen R, Wewer UM. (2003). ADAM12 induces actin cytoskeleton and extracellular matrix reorganization during early adipocyte differentiation by regulating beta1 integrin function. J Cell Sci. 116(Pt 19):3893-904.

Kleino I, Järviluoma A, Hepojoki J, Huovila AP, Saksela K. (2015). Preferred SH3 domain partners of ADAM metalloproteases include shared and ADAM-specific SH3interactions. PLoS One.10(3):e0121301.

Lafuste P, Sonnet C, Chazaud B, Dreyfus PA, Gherardi RK, Wewer UM, Authier FJ. (2005). ADAM12 and alpha9beta1 integrin are instrumental in human myogenic cell differentiation. Mol Biol Cell. 16(2):861-70.

Leung CT, Coulombe PA, Reed RR. (2007). Contribution of olfactory neural stem cells to tissue maintenance and regeneration. Nat Neurosci. 10(6):720-6.

Lledo PM, Merkle FT, Alvarez-Buylla A. (2008). Origin and function of olfactory bulb interneuron diversity. Trends Neurosci. 31(8):392-400.

Mackay-Sim A, Kittel P. (1991). Cell dynamics in the adult mouse olfactory epithelium: a quantitative autoradiographic study. J Neurosci. 11(4):979-84.

Makino N, Ookawara S, Katoh K, Ohta Y, Ichikawa M, Ichimura K. (2009). The morphological change of supporting cells in the olfactory epithelium after bulbectomy.Chem Senses. 34(2):171-9.

Mitchell KJ1, Pinson KI, Kelly OG, Brennan J, Zupicich J, Scherz P, Leighton PA, Goodrich LV, Lu X, Avery BJ, Tate P, Dill K, Pangilinan E, Wakenight P, Tessier-Lavigne M, Skarnes WC. (2001). Functional analysis of secreted and transmembrane proteins critical to mouse development.Nat Genet. 28(3):241-9.

Miragall F, Krause D, de Vries U, Dermietzel R. (1994). Expression of the tight junction protein ZO-1 in the olfactory system: presence of ZO-1 on olfactory sensory neurons and glial cells. J Comp Neurol. 341(4):433-48.

Mombaerts P. (2006). Axonal wiring in the mouse olfactory system. Annu Rev Cell Dev Biol. 22:713-37.

Ovadia J, Nie Q. (2013). Stem cell niche structure as an inherent cause of undulating epithelial morphologies. Biophys J. 104(1):237-46.

Potter SM, Zheng C, Koos DS, Feinstein P, Fraser SE, Mombaerts P. (2001). Structure and emergence of specific olfactory glomeruli in the mouse. J Neurosci. 21(24):9713-23.

Putnam AJ. (2014). The Instructive Role of the Vasculature in Stem Cell Niches.Biomater Sci. 2(11):1562-1573.

Rando TA, Chang HY. (2012). Aging, rejuvenation, and epigenetic reprogramming: resetting the aging clock. Cell. 148(1-2):46-57.

Reiss K, Maretzky T, Ludwig A, Tousseyn T, de Strooper B, Hartmann D, Saftig P. (2005). ADAM10 cleavage of N-cadherin and regulation of cell-cell adhesion and beta-catenin nuclear signaling. EMBO J. 24(4):742-52.

Riddle DR, Lichtenwalner RJ. Neurogenesis in the Adult and Aging Brain. In: Riddle DR, editor. Brain Aging: Models, Methods, and Mechanisms. Boca Raton (FL): CRC Press/Taylor & Francis; 2007. Chapter 6. Available from: http://www.ncbi.nlm.nih.gov/books/NBK3874/

Sagane K, Ohya Y, Hasegawa Y, Tanaka I. (1998). Metalloproteinase-like, disintegrin-like, cysteine-rich proteins MDC2 and MDC3: novel human cellular disintegrins highly expressed in the brain.Biochem J. 334 (Pt 1):93-8.

Sagane K, Ishihama Y, Sugimoto H. (2008). LGI1 and LGI4 bind to ADAM22, ADAM23 and ADAM11. Int J Biol Sci. 4(6):387-96.

Schindelin J, Arganda-Carreras I, Frise E, Kaynig V, Longair M, Pietzsch T, Preibisch S, Rueden C, Saalfeld S, Schmid B, Tinevez JY, White DJ, Hartenstein V, Eliceiri K, Tomancak P, Cardona A. (2012). Fiji: an open-source platform for biological-image analysis. Nat Methods. 9(7):676-82.

Schnittke N, Herrick DB, Lin B, Peterson J, Coleman JH, Packard AI, Jang W, Schwob JE. (2015). Transcription factor p63 controls the reserve status but not the stemness of horizontal basal cells in the olfactory epithelium. Proc Natl Acad Sci U S A. 112(36):E5068-77.

Schwob JE, Youngentob SL, Mezza RC. (1995). Reconstitution of the rat olfactory epithelium after methyl bromide-induced lesion. J Comp Neurol. 359(1):15-37.

Seppälä EH, Jokinen TS, Fukata M, Fukata Y, Webster MT, Karlsson EK, Kilpinen SK, Steffen F, Dietschi E, Leeb T, Eklund R, Zhao X, Rilstone JJ, Lindblad-Toh K, Minassian BA, Lohi H. (2011). LGI2 truncation causes a remitting focal epilepsy in dogs. PLoS Genet. 7(7):e1002194.

Shetty RS, Bose SC, Nickell MD, McIntyre JC, Hardin DH, Harris AM, McClintock TS. (2005). Transcriptional changes during neuronal death and replacement in the olfactory epithelium. Mol Cell Neurosci. 30(4):583-600.

Sun YP, Deng KJ, Wang F, Zhang J, Huang X, Qiao S, Zhao S. (2004). Two novel isoforms of Adam23 expressed in the developmental process of mouse and human brains. Gene. 325:171-8.

Sun Y, Wang Y, Zhang J, Tao J, Wang C, Jing N, Wu C, Deng K, Qiao S. (2007). ADAM23 plays multiple roles in neuronal differentiation of P19 embryonal carcinoma cells. Neurochem Res. 32(7):1217-23.

Sun C, Wu MH, Guo M, Day ML, Lee ES, Yuan SY. (2010). ADAM15 regulates endothelial permeability and neutrophil migration via Src/ERK1/2 signaling. Cardiovasc Res. 87(2):348-55.

Suzuki J, Yoshizaki K, Kobayashi T, Osumi N.Neural crest-derived horizontal basal cells as tissue stem cells in the adult olfactory epithelium. (2013). Neurosci Res.75(2):112-20.

Tanaka M, Nanba D, Mori S, Shiba F, Ishiguro H, Yoshino K, Matsuura N, Higashiyama S. (2004). ADAM binding protein Eve-1 is required for ectodomain shedding of epidermal growth factor receptor ligands. J Biol Chem. 279(40):41950-9.

Verbisck NV, Costa ET, Costa FF, Cavalher FP, Costa MD, Muras A, Paixão VA, Moura R, Granato MF, Ierardi DF, Machado T, Melo F, Ribeiro KB, Cunha IW,Lima VC, Maciel Mdo S, Carvalho AL, Soares FF, Zanata S, Sogayar MC, Chammas R, Camargo AA. (2009). ADAM23 negatively modulates alpha(v)beta(3) integrin activation during metastasis. Cancer Res. 69(13):5546-52.

Wang Y, Sun Y, Qiao S. (2012). ADAM23 knockdown promotes neuronal differentiation of P19 embryonal carcinoma cells by up-regulating P27KIP1 expression. Cell Biol Int. 36(12):1275-9.

Whitman MC, Greer CA. (2009). Adult neurogenesis and the olfactory system. Prog Neurobiol. 89(2):162-75.

Wolfsberg TG, Straight PD, Gerena RL, Huovila AP, Primakoff P, Myles DG, White JM. (1995). ADAM, a widely distributed and developmentally regulated gene family encoding membrane proteins with a disintegrin and metalloprotease domain. Dev Biol. 169(1):378-83.

Yang P, Baker KA, Hagg T. (2005). A disintegrin and metalloprotease 21 (ADAM21) is associated with neurogenesis and axonal growth in developing and adult rodent CNS. J Comp Neurol. 490(2):163-79.

Yavari R, Adida C, Bray-Ward P, Brines M, Xu T. (1998). Human metalloprotease-disintegrin Kuzbanian regulates sympathoadrenal cell fate in development and neoplasia. Hum Mol Genet. 7(7):1161-7.

Yoshihara Y, Kawasaki M, Tamada A, Fujita H, Hayashi H, Kagamiyama H, Mori K. (1997). OCAM: A new member of the neural cell adhesion molecule family related to zone-to-zone projection of olfactory and vomeronasal axons. J Neurosci. 17(15):5830-42.

VITA

Elaine Orendorff was raised in Geneseo, IL. She attended the University of Illinois, Urbana-Champaign, graduating in 2012 with a Bachelor of Science degree in Integrative Biology (Honors) with a minor in Chemistry. She worked for two years prior to starting the Master's in Biology program at Loyola University Chicago. She was supported throughout her studies by a fellowship award from Loyola's Graduate School. Starting this Fall, she will pursue a doctorate degree abroad in the École des Neurosciences de Paris, Île-de-France graduate program.